Supporting Information

for

CuAAC "click" Active Template Synthesis of Functionalized [2]Rotaxanes Using Small *exo*-Substituted Macrocycles: How small is too small?

Asif Noor, Warrick K. C. Lo, Stephen C. Moratti and James D. Crowley*

Department of Chemistry, University of Otago, PO Box 56, Dunedin, New Zealand

E-mail: jcrowley@chemistry.otago.ac.nz,

Fax: +64 3 479 7906,

Tel: +64 3 479 7731.

Contents

1 General Experimental Section

Unless otherwise stated, all reagents were purchased from commercial sources and used without further purification. Dry dichloromethane (CH_2Cl_2) and acetonitrile (CH_3CN) were obtained by passing the solvents through an activated alumina column on a PureSolvTM solvent purification system (Innovative Technologies, Inc., MA). 3,5-Dihydroxybenzyl alcohol[1, 2] and 2,6-di(*p*-bromomethylphenoxymethyl)pyridine[3] were prepared according to literature procedures. Petrol refers to the fraction of petroleum ether boiling in the range 40-60 °C. Flash column chromatography was carried out using Kiesegel C60 (Fisher) as the stationary phase. Analytical TLC was performed on pre-coated silica gel plates (0.25 mm thick, 60F254, Merck, Germany) and observed under UV light. All melting points were determined using a Sanyo Gallenkamp apparatus and are uncorrected. ^{1}H, $^{13}C\{^{1}H\}$, ^{1}H DOSY, COSY, NOESY, and ROESY NMR spectra were recorded either on a 400 MHz Varian/Agilent 400-MR or Varian/Aglient 500 MHz AR spectrometer at 298 K. Chemical shifts are reported in parts per million (ppm) and referenced to residual solvent peak. Coupling constants (*J*) are reported in Hertz (Hz). Standard abbreviations indicating multiplicity were used as follows: m = multiplet, quint. = quintet, q = quartet, t = triplet, d = doublet, s = singlet, br = broad, ABq = AB quartet. Microanalyses were performed at the Campbell Microanalytical Laboratory at University of Otago. High resolution electrospray ionization mass spectra (HR-ESMS) were collected on a Bruker micrOTOF-Q spectrometer.

Safety note: Low molecular weight organic azides are potential explosives, care must be taken when handling.[4] A standard PVC blast shield was used when necessary. Additionally, copper azides and acetylides are explosive when dry, and their traces should be removed before the CuAAC reaction products are dried.

2 Experimental Procedures

2.1 Macrocycles Synthesis

2.1.1 Dibromide 3

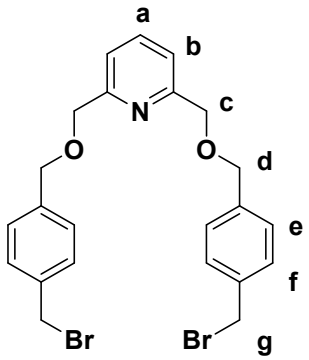

A suspension of 2,6-pyridinedimethanol (0.50 g, 3.6 mmol), 1,4-bis(bromomethyl)benzene (2.85 g, 10.8 mmol) and NaH (0.259 g, 10.8 mmol, 95% powder) in dry THF (200 mL) was stirred for 24 h at room temperature (RT) under a nitrogen atmosphere. Methanol (10 mL) was then added and the mixture was stirred for 5 min. The solvents were removed under reduced pressure. The residue was dissolved in CH_2Cl_2 and washed with water (3 × 20 mL) and brine (20 mL). The solvent of the organic layer was removed under reduced pressure and the resulting residue was purified by column chromatography (silica gel, ethyl acetate/petrol, 1:1) to give **3** (450 mg, 25%) as yellow solid. ^{1}H NMR (400 MHz, $CDCl_3$) δ 7.72 (t, J = 7.7 Hz, 1H, H_a), 7.41 – 7.34 (m, 10H, H_b, H_e, H_f), 4.67 (s, 4H, H_c), 4.64 (s, 4H, H_d), 4.50 (s, 4H, H_g); ^{13}C NMR (100 MHz, $CDCl_3$) δ 157.93, 138.53, 137.48, 137.40, 129.30, 128.27, 120.21, 73.32, 72.60, 33.42; HR-ESMS: *m/z* = 527.9969 [**3**+Na]$^+$ (calc. for $C_{23}H_{23}Br_2NNaO_2$, 527.9921); Anal. calc. for $C_{23}H_{23}Br_2NO_2$: C, 54.68; H, 4.59; N, 2.77; found: C, 54.87; H, 4.76, N, 2.68.

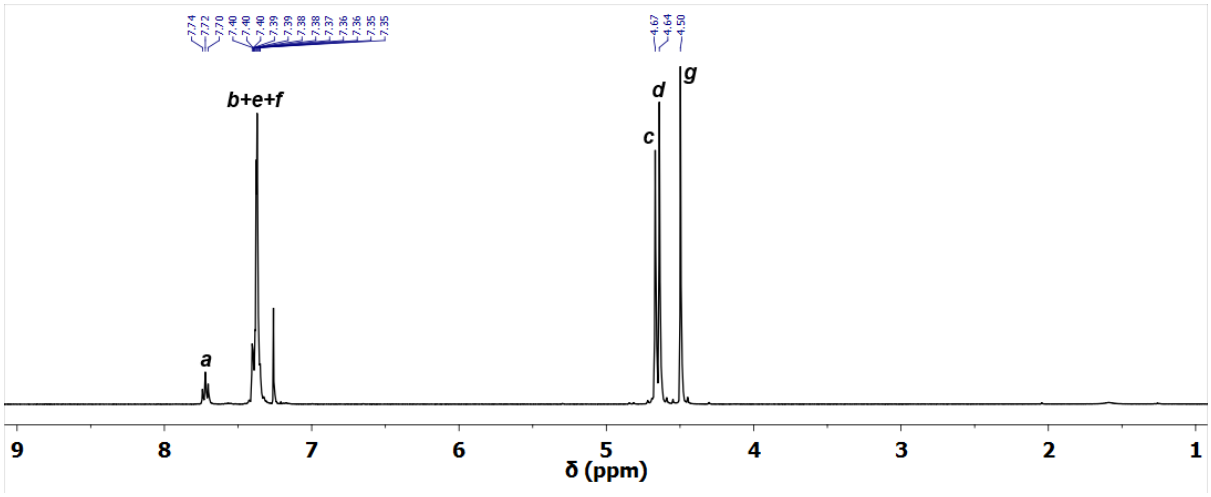

Figure S1. ^{1}H NMR spectrum (400 MHz, $CDCl_3$, 298 K) of **3**.

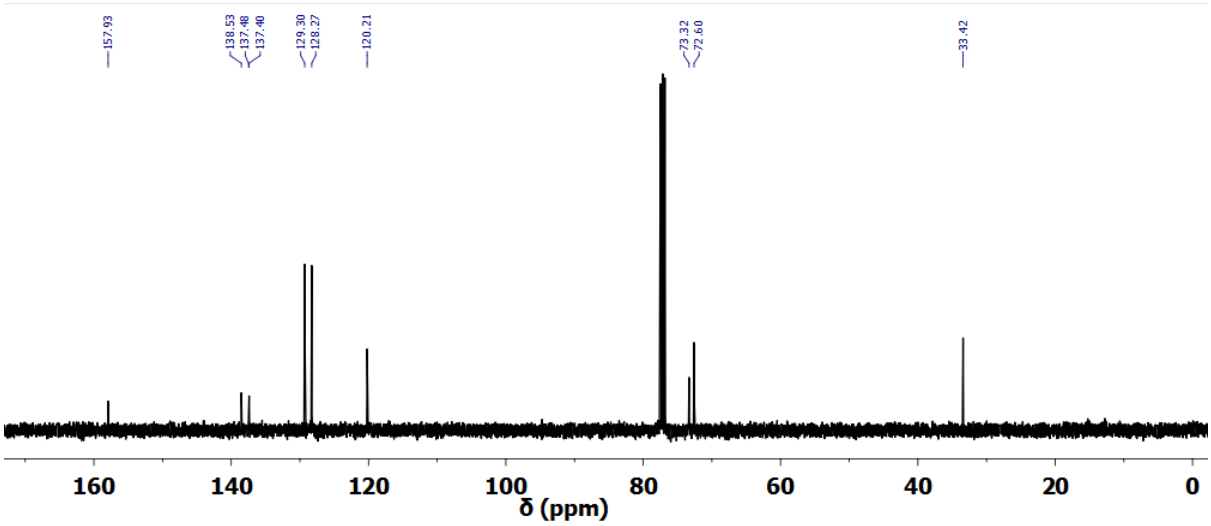

Figure S2. ^{13}C NMR spectrum (100 MHz, $CDCl_3$, 298 K) of **3**.

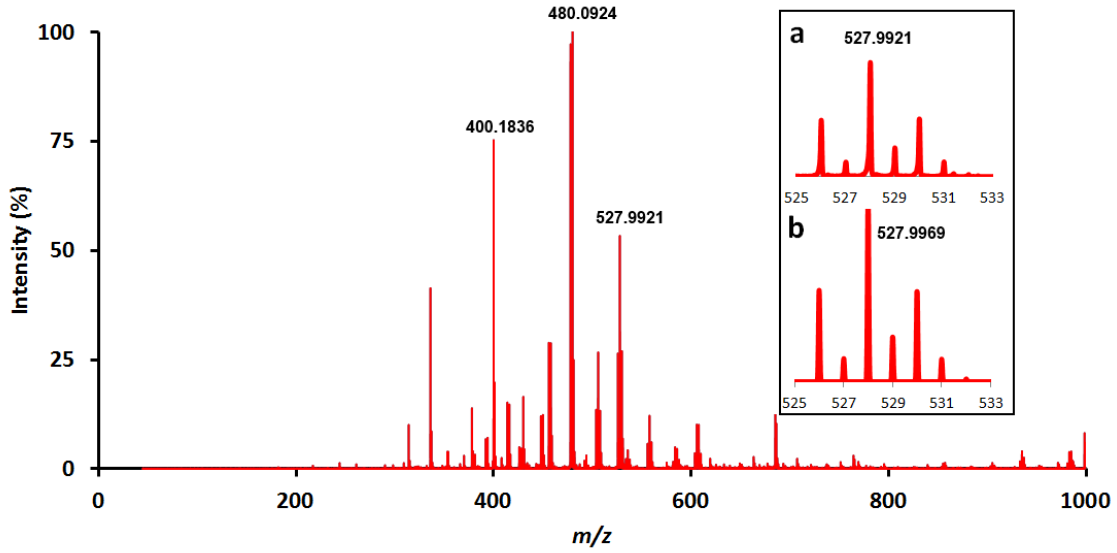

Figure S3. HR-ESMS spectrum of **3**, inset a) observed and b) calculated isotopic patterns for [**3**+Na]$^+$ at *m/z* = 527.9921. Also showing peaks due to [**3**-Br+OCH_3+Na]$^+$ at *m/z* = 480.0924 and [**3**-$(Br)_2$+OCH_3+Na+H]$^+$ at *m/z* = 400.1836.

2.1.2 Macrocycle 4

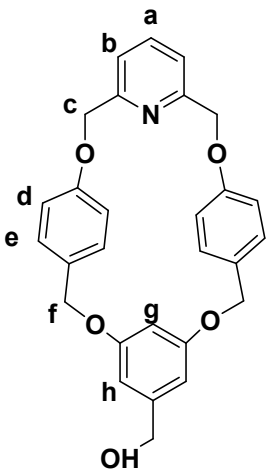

Under a nitrogen atmosphere, the dibromide **2**[2] (2.00 g, 4.19 mmol) and 3,5-dihydroxybenzyl alcohol (587 mg, 4.19 mmol) were added slowly via dropping funnels to a suspension of K_2CO_3 (11.5 g, 84 mmol) in acetone at 55 °C over a period of 12 h. The reaction mixture was refluxed for 48 h, then cooled to RT and filtered to remove the suspended colourless solids. The solvent was removed under reduced pressure and the resulting residue was dissolved in CH_2Cl_2 (50 mL) and washed with water (3 × 20 mL) and brine (20 mL). The solvent of the

organic layer was removed under reduced pressure. The solid obtained was dissolved in chloroform (1 mL). Addition of methanol to this solution resulted in the precipitation of a colourless solid. The precipitate was collected by filtration and dried to afford macrocycle **4** (508 mg, 26%). ^{1}H NMR (400 MHz, $CDCl_3$) δ 7.63 (t, J = 7.7 Hz, 1H, H_a), 7.32 (d, J = 7.7 Hz, 2H, H_b), 7.02 (d, J = 8.9 Hz, 4H, H_d), 6.83 (d, J = 8.9 Hz, 4H, H_e), 6.45 (d, J = 2.2 Hz, 2H, H_h), 6.42 (t, J = 2.3 Hz, 1H, H_g), 5.25 (s, 4H, H_c), 5.07 (s, 4H, H_f), 4.49 (d, J = 5.9 Hz, 2H, H_i); ^{13}C NMR (100 MHz, $CDCl_3$) δ 159.34, 157.73, 157.04, 143.57, 138.06, 129.53, 128.37, 122.25, 115.26, 108.28, 100.11, 70.81, 69.06, 65.21; IR ν(cm^{-1}) 3162, 2886, 1611, 1510, 1554; HR-ESMS: *m/z* = 478.4625 [**4**+Na]$^{+}$ (calc. for $C_{28}H_{25}NNaO_5$, 478.1632); Anal. calc. for $C_{28}H_{25}NO_5$•0.5(CH_3OH): C, 72.60; H, 5.77; N, 2.97; found: C, 72.56; H, 5.82, N, 2.88.

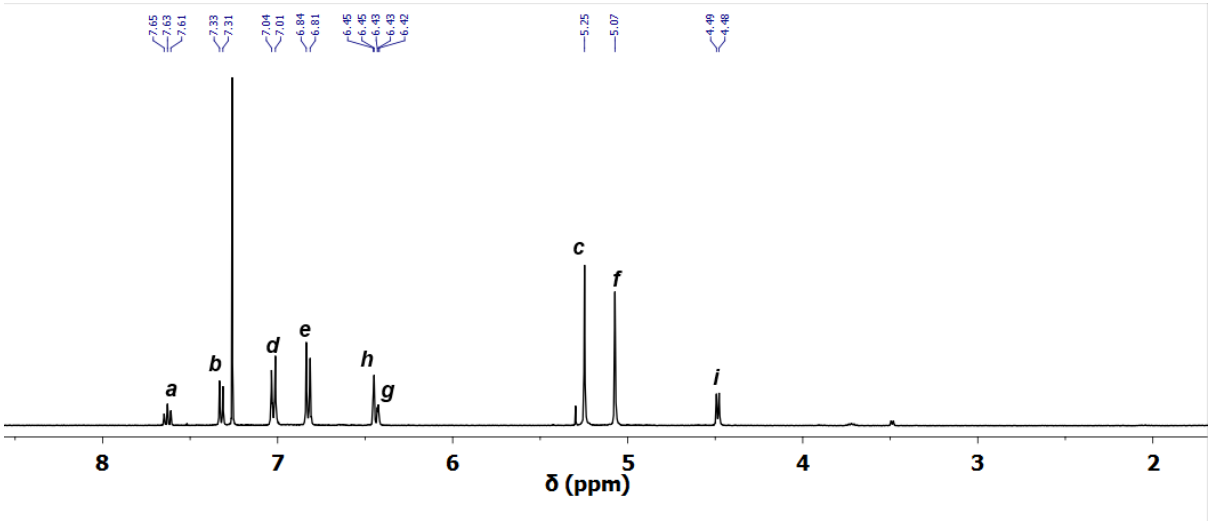

Figure S4. ^{1}H NMR spectrum (400 MHz, $CDCl_3$, 298 K) of **4**.

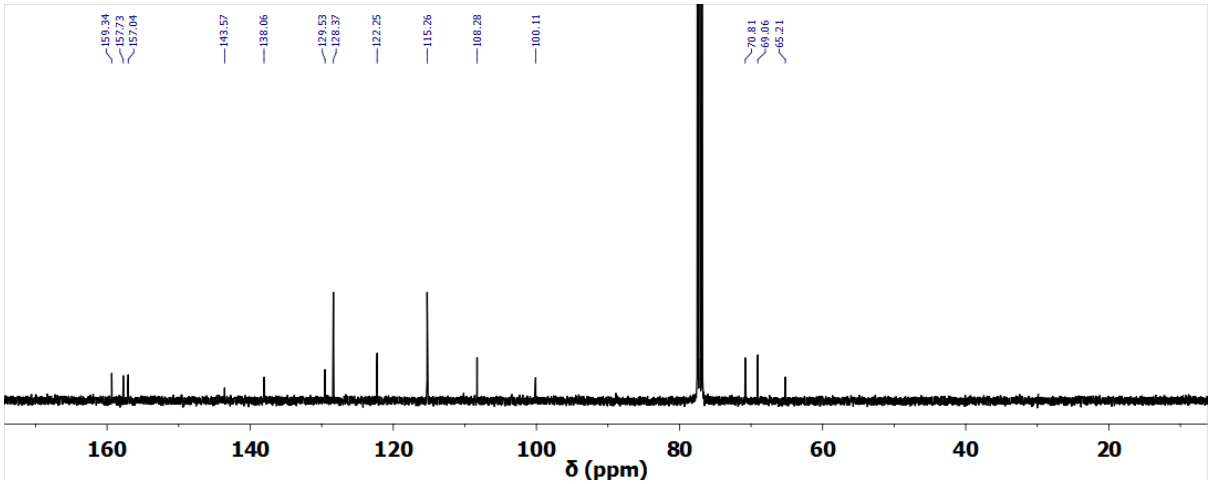

Figure S5. ^{13}C NMR spectrum (100 MHz, $CDCl_3$, 298 K) of **4**.

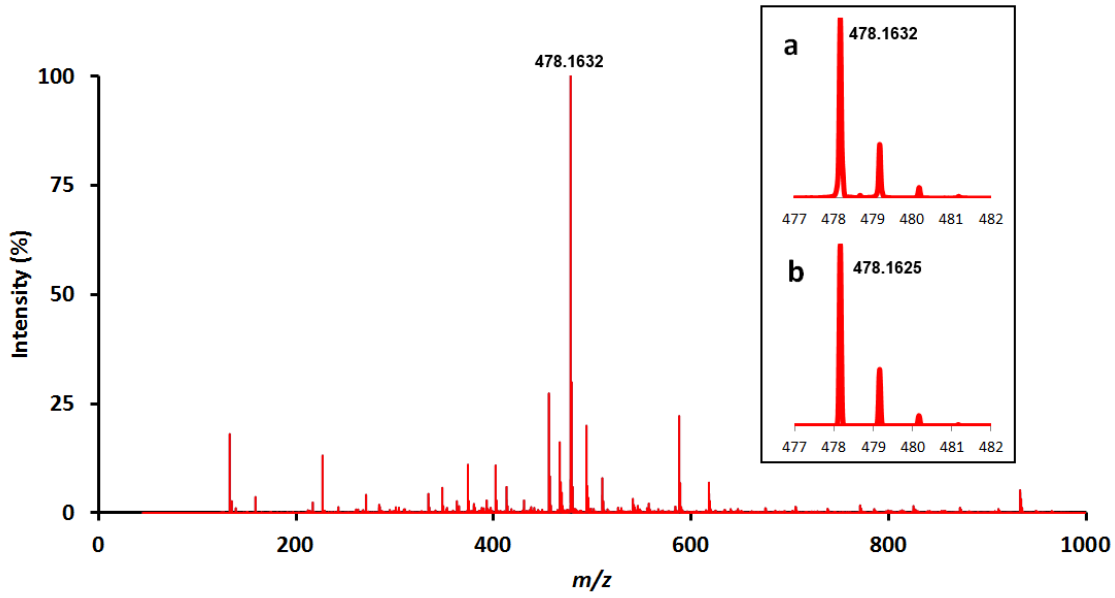

Figure S6. HR-ESMS spectrum of **4**, inset a) observed and b) calculated isotopic patterns for [**4**+Na]$^+$ at *m/z* = 478.1632.

2.1.3 Macrocycle 5

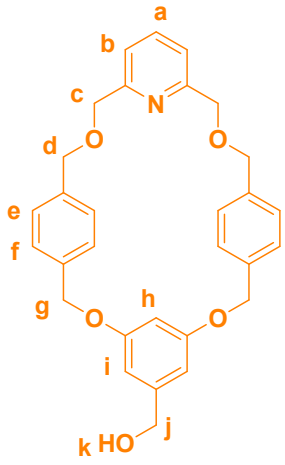

Under a nitrogen atmosphere, solutions of dibromide **3** (0.400 g, 0.792 mmol) and 3,5-dihydroxybenzyl alcohol (0.111 g, 0.792 mmol) in acetone (50 mL) were added slowly via 50 mL syringes to a suspension of K_2CO_3 (1.10 g, 7.92 mmol) in acetone at 50 °C over a period of 48 h. The reaction mixture was refluxed for 48 h, then cooled to RT and filtered to remove the suspended colourless solids. The solvent was removed under reduced pressure. The residue was dissolved in CH_2Cl_2 (50 mL) and washed with water (3 × 20 mL) and brine (20 mL). The solvent of the organic layer was removed under reduced pressure. The solid obtained was dissolved in a minimum amount of CH_2Cl_2. Addition of methanol to this solution resulted in the precipitation of a colourless solid. The precipitate was filtered and dried to afford macrocycle **5** (120 mg, 31%). ^{1}H NMR (400 MHz, DMSO-d_6) 7.79 (t, J = 7.7 Hz, 1H, H_a), 7.44 – 7.27 (m, 10H, H_b, H_e, H_f), 6.56 (d, J = 2.6 Hz, 2H, H_i), 6.42 (t, J = 2.2 Hz, 1H, H_h), 5.15 (t, J = 5.9 Hz, 1H, H_k), 5.05 (s, 4H, H_c), 4.58 (s, 4H, H_d), 4.54 (s, 4H, H_g), 4.41 (d, J = 5.8 Hz, 2H, H_j); ^{13}C NMR (100 MHz, DMSO-d_6) δ 159.13, 157.42, 145.19, 137.61, 137.41, 136.46, 127.72, 127.49, 120.12, 105.30, 100.28, 72.28, 71.53, 68.79, 62.77; IR ν(cm^{-1}) 3416, 2918, 2849, 1610, 1592, 1561; HR-ESMS: m/z = 484.2118 $[(\mathbf{5})_2+2H]^{2+}$

(calc. for $C_{60}H_{60}N_2O_{10}$, 484.2144); Anal. calc. for $C_{30}H_{29}NO_5$: C, 74.52; H, 6.04; N, 2.90; found: C, 74.27; H, 5.93, N, 2.90.

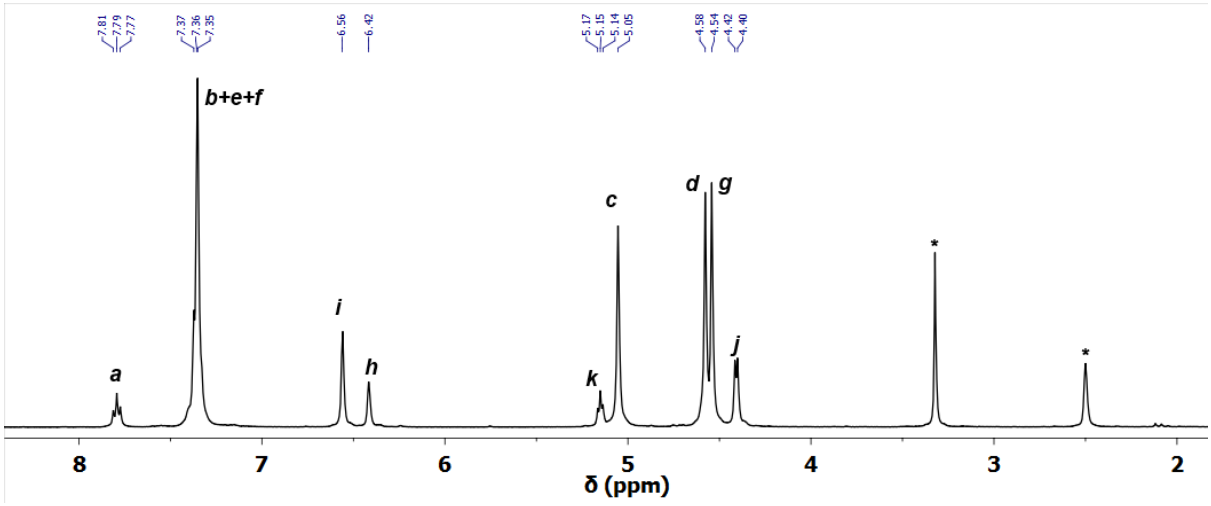

Figure S7. ^{1}H NMR spectrum (400 MHz, DMSO-d_6, 298 K) of **5** (* peaks due to DMSO and H_2O).

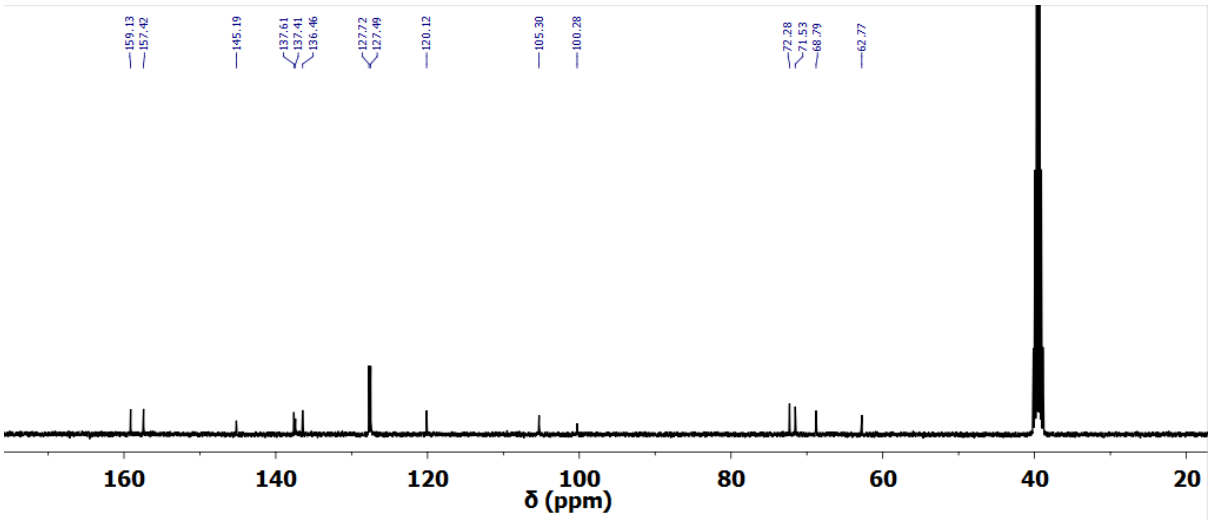

Figure S8. ^{13}C NMR spectrum (100 MHz, DMSO-d_6, 298 K) of **5**.

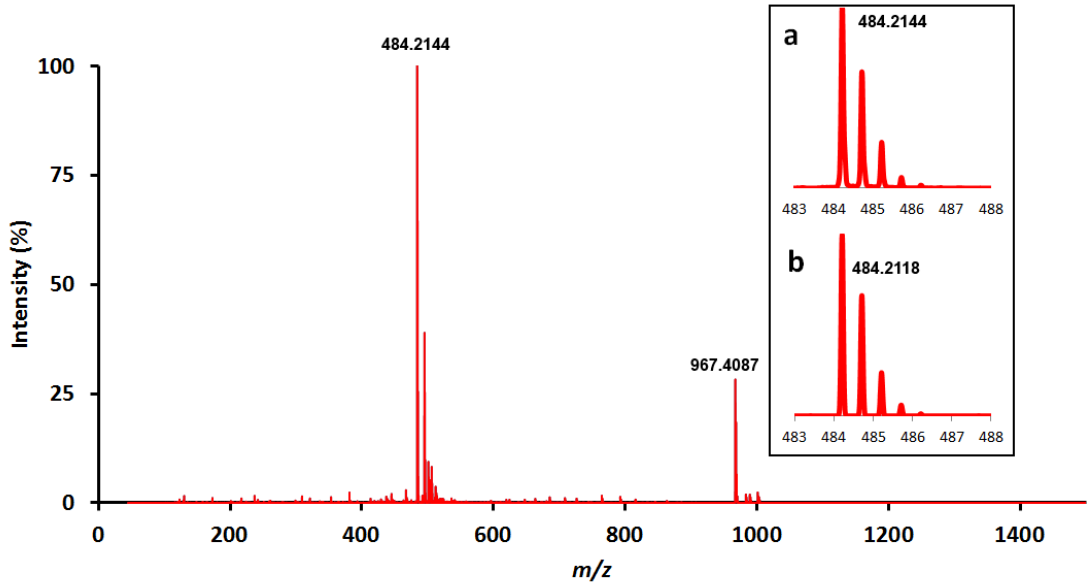

Figure S9. HR-ESMS spectrum of **5**, inset a) observed and b) calculated isotopic patterns for $[(\mathbf{5})_2+2H]^{2+}$ at *m/z* = 484.2144. Also showing peaks due to $[(\mathbf{5})_2+H]^{+}$ at *m/z* = 967.4087.

2.2 CuAAC Active Metal Template Synthesis of [2]Rotaxanes

2.2.1 Rotaxane 8

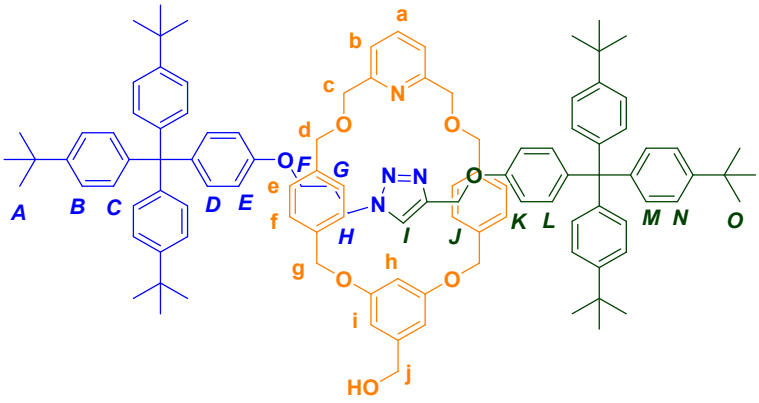

A solution of macrocycle **5** (50 mg, 0.10 mmol) and $[Cu(CH_3CN)_4](PF_6)$ (43 mg, 0.11 mmol) in dry CH_2Cl_2 (10 mL) was stirred under nitrogen for 1 h. The azide **6**[4] (304 mg, 0.517 mmol) and alkyne **7**[4] (281 mg, 0.157 mmol) stoppers were then added. The resulting mixture was refluxed for 48 h, then diluted with CH_2Cl_2 (10 mL). A methanol (20 mL) solution of KCN (68 mg, 1.0 mmol) was added and the resulting suspension was stirred at RT for 2 h. The

solvents were evaporated by heating the mixture at 80°C in an oil bath. The residue was partitioned between water (50 mL) and CH_2Cl_2 (75 mL) and the layers were separated. The aqueous layer was extracted with CH_2Cl_2 (2 × 75 mL) and the combined organic layers were washed with water (50 mL) and brine (50 mL). After drying the organic layer over $MgSO_4$, the solvent was removed under reduced pressure. The residue was purified by column chromatography (silica gel, ethyl acetate/petrol, 1:1) to give rotaxane **8** as colourless solid (40 mg, 17%). The reaction was repeated at 80 °C in a sealed tube to afford rotaxane **8** in 70% yield. ^{1}H NMR (400 MHz, $CDCl_3$) δ 7.89 (s, 1H, H_I), 7.45 (t, *J* = 7.7 Hz, 1H, H_a), 7.32 – 7.00 (m, 34H, H_B, H_C, H_D, H_L, H_M, H_N, H_b, H_f), 6.83 (d, *J* = 8.5 Hz, 2H, H_K), 6.73 (d, *J* = 7.7 Hz, 4H, H_e), 6.68 (d, *J* = 2.3 Hz, 2H, H_i), 6.41 (d, *J* = 8.8 Hz, 2H, H_E), 6.30 (t, *J* = 2.3 Hz, 1H, H_h), 5.09 and 5.00 (ABq, *J* = 13.2 Hz, 4H, H_g), 4.93 (s, 2H, H_J), 4.53 (s, 2H, H_j), 4.43 and 4.41 (ABq, *J* = 10.2 Hz, 4H, H_c), 4.30 and 4.20 (ABq, *J* = 10.5 Hz, 4H, H_d), 2.37 (t, *J* = 7.0 Hz, 2H, H_F), 2.19 – 2.08 (m, 2H, H_H), 1.32 (s, 27H, H_A or H_O), 1.28 (s, 27H, H_O, H_A or H_O), 0.17 – 0.04 (m, 2H, H_G); ^{13}C NMR (100 MHz, $CDCl_3$)* δ 158.55, 157.03, 156.77, 156.31, 148.44, 144.80, 144.54, 144.22, 142.96, 140.08, 138.94, 137.65, 137.24, 136.30, 132.36, 132.01, 130.91, 130.83, 129.83, 129.15, 124.58, 124.21, 124.18, 122.36, 113.49, 113.46, 106.48, 104.30, 73.78, 73.20, 68.03, 65.17, 64.45, 63.29, 63.20, 61.90, 45.57, 34.47, 34.43, 31.57, 31.52, 29.52 (*28 out of 29 ^{13}C resonances were observed in aromatic region possibly due to overlapping of signals); IR *ν*(cm^{-1}) 2961, 2950. 2886, 1605, 1593, 1503; HR-ESMS: *m/z* = 1636.9395 [**8**+Na]$^+$ (calc. for $C_{110}H_{124}N_4NaO_7$, 1636.9456); Anal. calc. for $C_{110}H_{124}N_4O_7$: C, 80.94; H, 7.74; N, 3.47; found: C, 80.94; H, 7.97, N, 3.30.

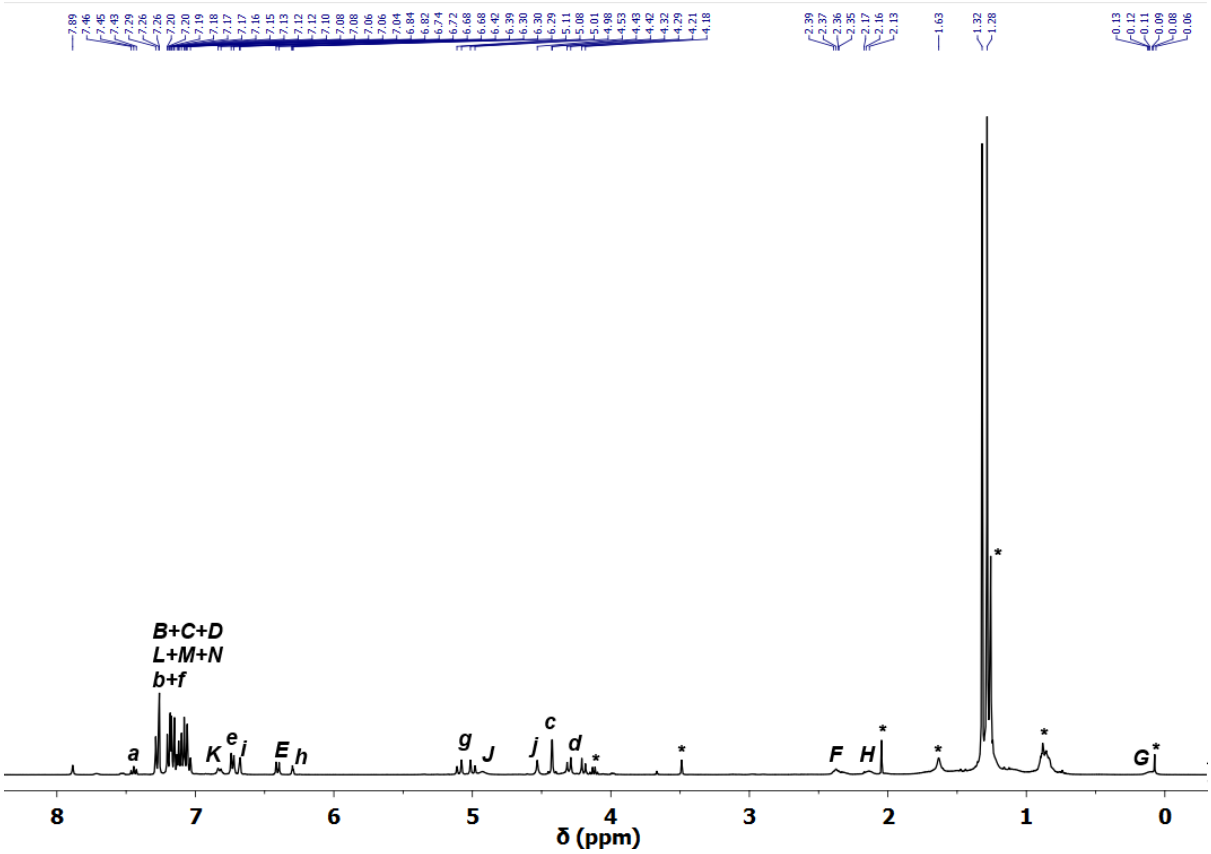

Figure S10. ^{1}H NMR spectrum (400 MHz, $CDCl_3$, 298 K) of **8** (* peaks due to grease, H_2O, ethyl acetate and *n*-hexane).

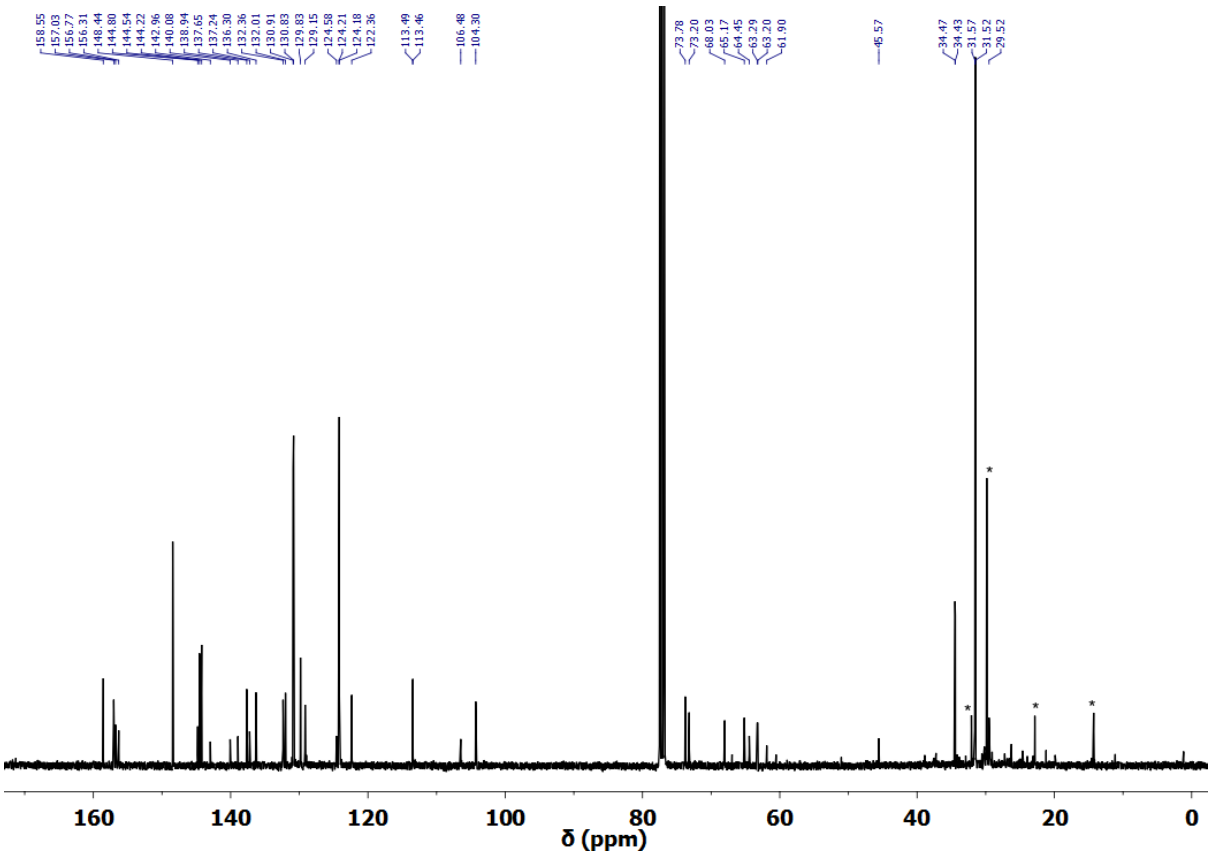

Figure S11. ^{13}C NMR spectrum (100 MHz, $CDCl_3$, 298 K) of **8** (* peaks due to grease, ethyl acetate and *n*-hexane).

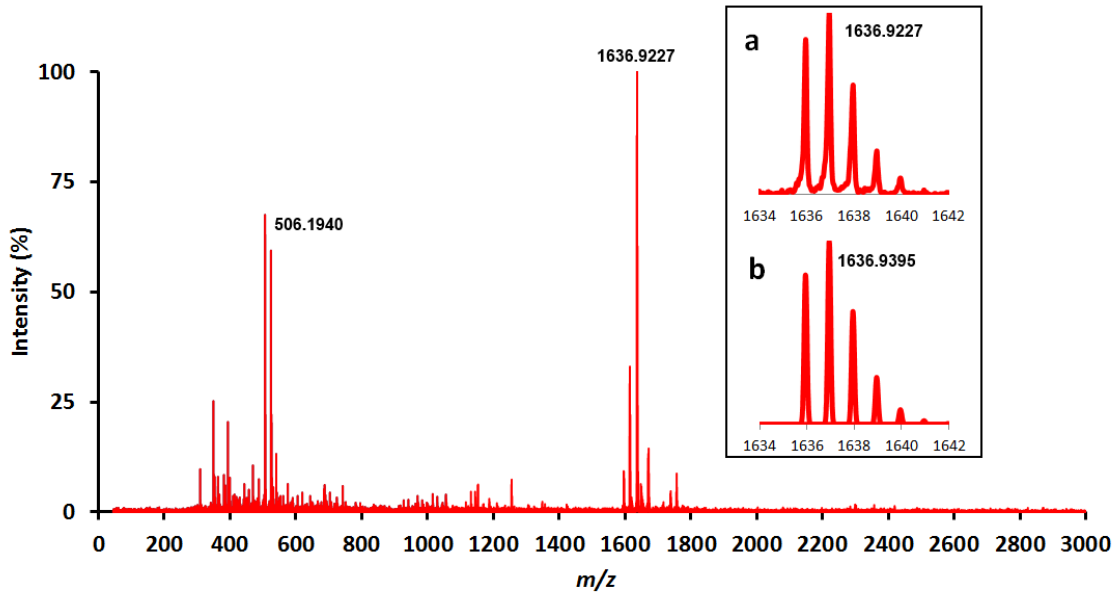

Figure S12. HR-ESMS spectrum of **8**, inset a) observed and b) calculated isotopic patterns for [**8**+Na]$^+$ at *m/z* = 1636.9227. Also showing peaks due to [**5**+Na]$^+$ at *m/z* = 506.1940.

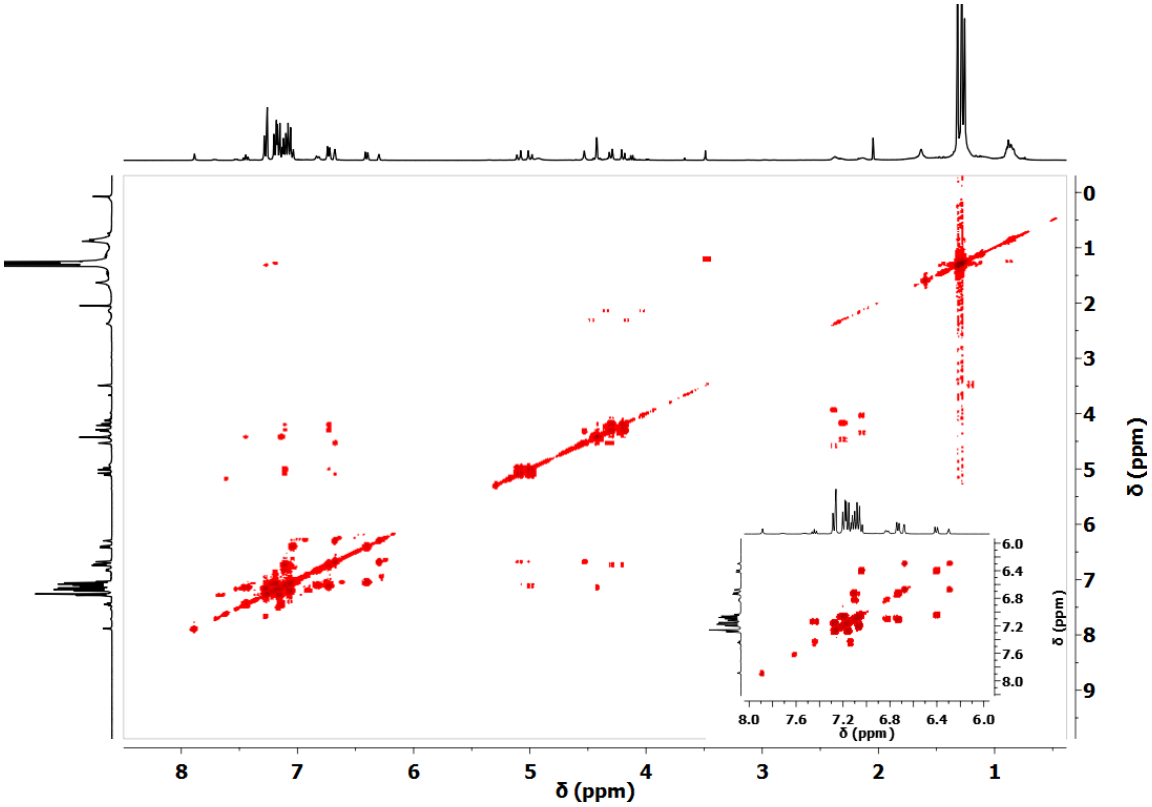

Figure S13. ^{1}H COSY NMR spectrum (400 MHz, $CDCl_3$, 298 K) of **8**.

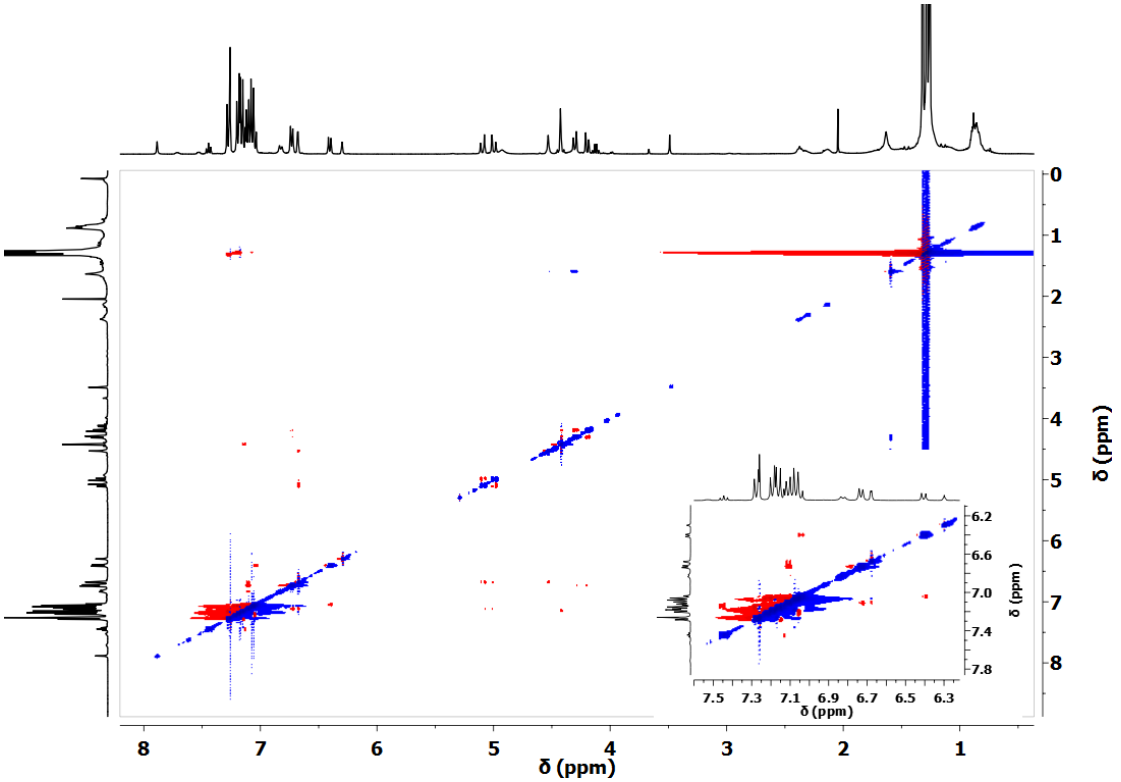

Figure S14. ^{1}H ROESY NMR spectrum (400 MHz, $CDCl_3$, 298 K) of **8**.

2.2.2 Rotaxane 11

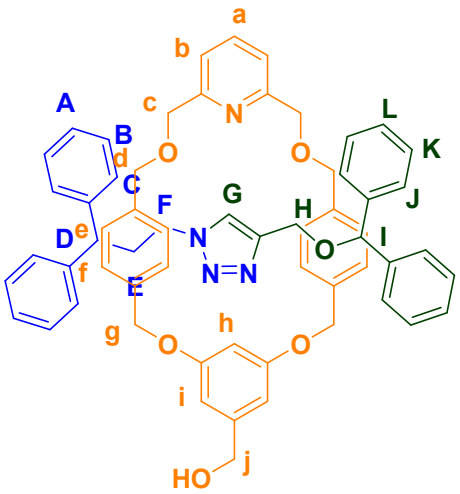

A solution of macrocycle **5** (35 mg, 0.072 mmol), $[Cu(CH_3CN)_4](PF_6)$ (27 mg, 0.072 mmol), azide **9**[5] (86 mg, 0.362 mmol) and alkyne **10**[6] (80 mg, 0.362 mmol) in dry CH_2Cl_2 (10 mL) was heated at 80 °C in a sealed tube for 72 h. After cooling the mixture to RT, the mixture was diluted with CH_2Cl_2 (10 mL) and a methanol (20 mL) solution of KCN (47 mg, 0.72 mmol) was added. The resulting suspension was stirred at RT for 2 h, and then the solvents were evaporated by heating the mixture at 80 ^{0}C in an oil bath. The residue was purified in the same way as reported (above) for rotaxane **8**, to afford rotaxane **11** as colourless solid (36 mg, 52%). ^{1}H NMR (400 MHz, $CDCl_3$) δ 8.35 (s, 1H, H_G), 7.74 (t, J = 7.7 Hz, 1H, H_a), 7.49 – 7.43 (m, 4H, H_J), 7.38 – 7.10 (m, 14H, H_A, H_B, H_K, H_L, H_b), 6.84 (d, J = 2.3 Hz, 2H, H_J), 6.78 (d, J = 7.9 Hz, 4H, H_f), 6.74 (d, J = 6.4 Hz, 4H, H_C), 6.43 (t, J = 2.3 Hz, 1H, H_h), 6.29 (d, J = 7.7 Hz, 4H, H_e), 5.63 (s, 1H, H_I), 5.18 and 4.82 (ABq, J = 13.0 Hz, 4H, H_g), 4.72 (s, 2H, H_j), 4.57 (s, 2H, H_H), 4.44 and 4.42 (ABq, J = 10.1 Hz, 4H, H_c), 4.21 and 3.98 (ABq, J = 9.8 Hz, 4H, H_d), 2.87 (t, J = 7.8 Hz, 1H, H_D), 1.87 – 1.77 (m, 2H, H_F), 0.77 – 0.66 (m, 2H, H_E); ^{13}C NMR (100 MHz, $CDCl_3$) 159.06, 157.31, 144.58, 143.78, 142.49, 137.44, 136.57, 136.30, 129.80, 129.07, 128.44, 128.21, 128.19, 127.53, 127.39, 127.27, 125.96, 122.47, 106.28, 106.24, 82.63, 73.94, 73.74, 68.23, 66.38, 62.52, 50.17, 48.29, 47.42, 36.02; IR ν(cm$^-$

[1]) 3058, 2921. 2850, 1591, 1493, 1451; HR-ESMS: *m/z* = 965.4249 [**11**+Na]$^+$ (calc. for $C_{61}H_{58}N_4NaO_6$, 965.4228).

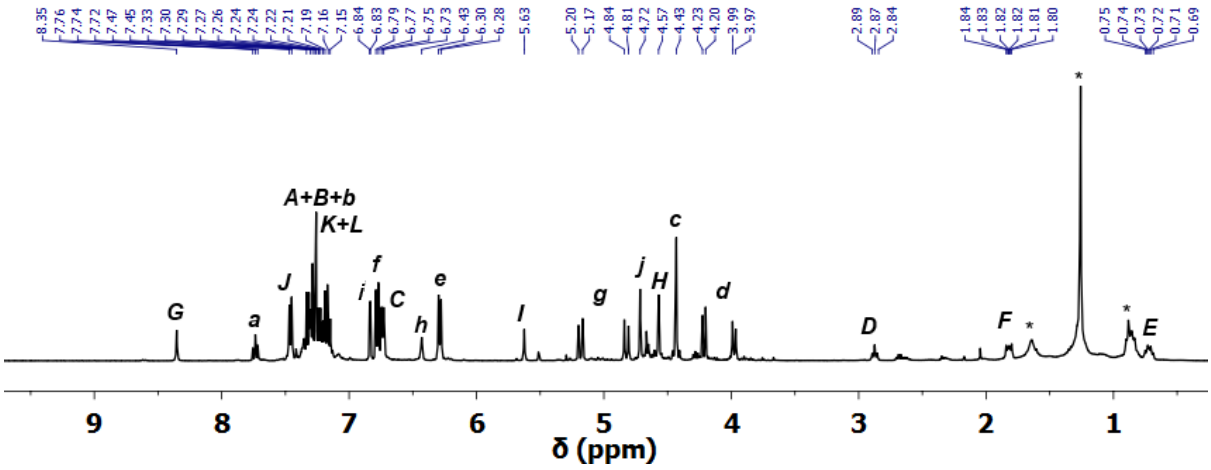

Figure S15. [1]H NMR spectrum (400 MHz, $CDCl_3$, 298 K) of **11** (* peaks due to grease, H_2O and *n*-hexane).

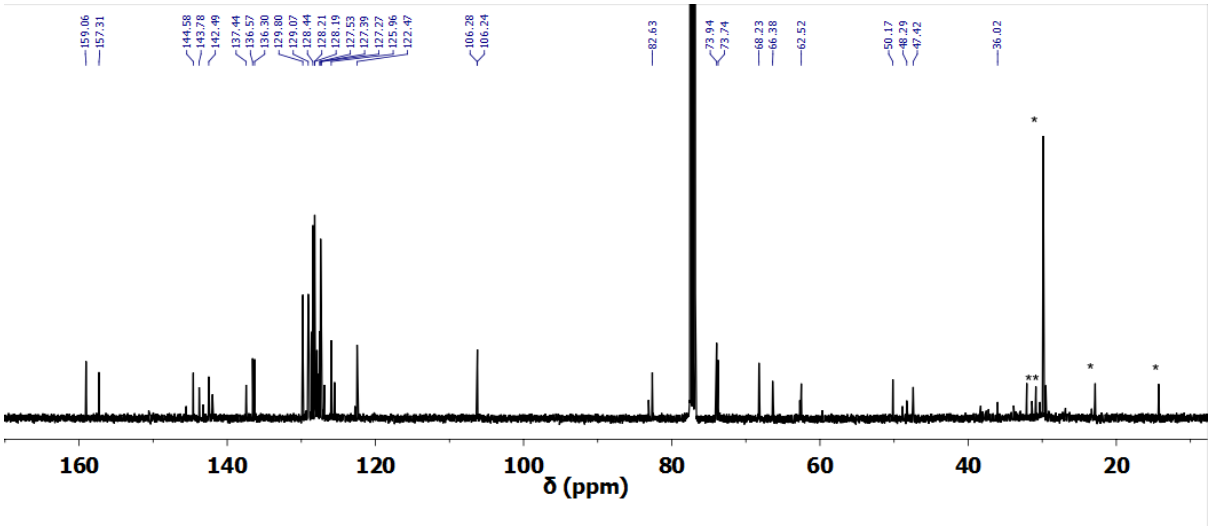

Figure S16. [13]C NMR spectrum (100 MHz, $CDCl_3$, 298 K) of **11** (* peaks due to grease, ethyl acetate and *n*-hexane).

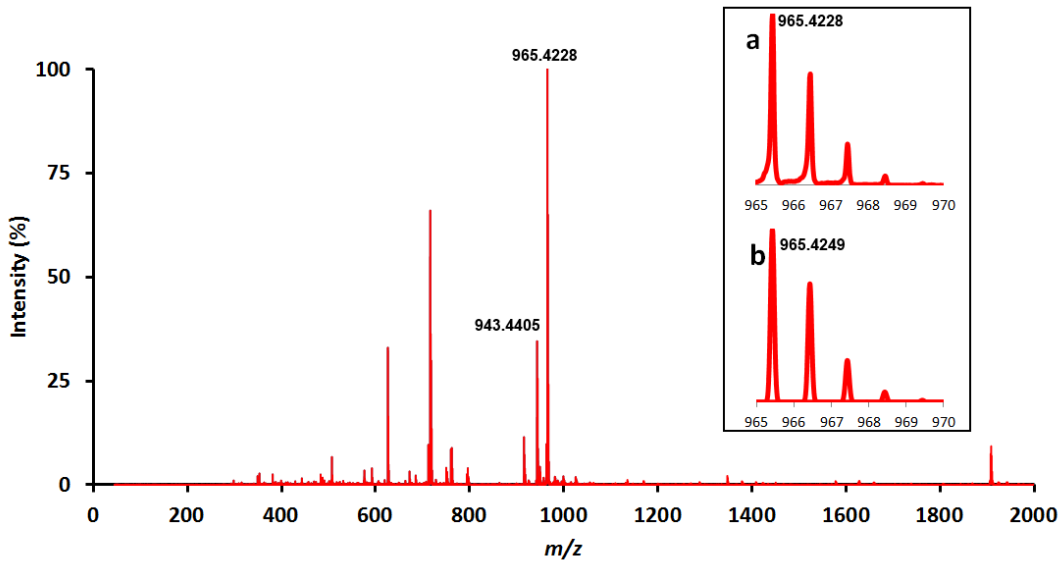

Figure S17. HR-ESMS spectrum of **11**, inset a) observed and b) calculated isotopic patterns for [**11**+Na]$^+$ at *m/z* = 965.4228. Also showing peaks due to [**11**+H]$^+$ at 943.4405.

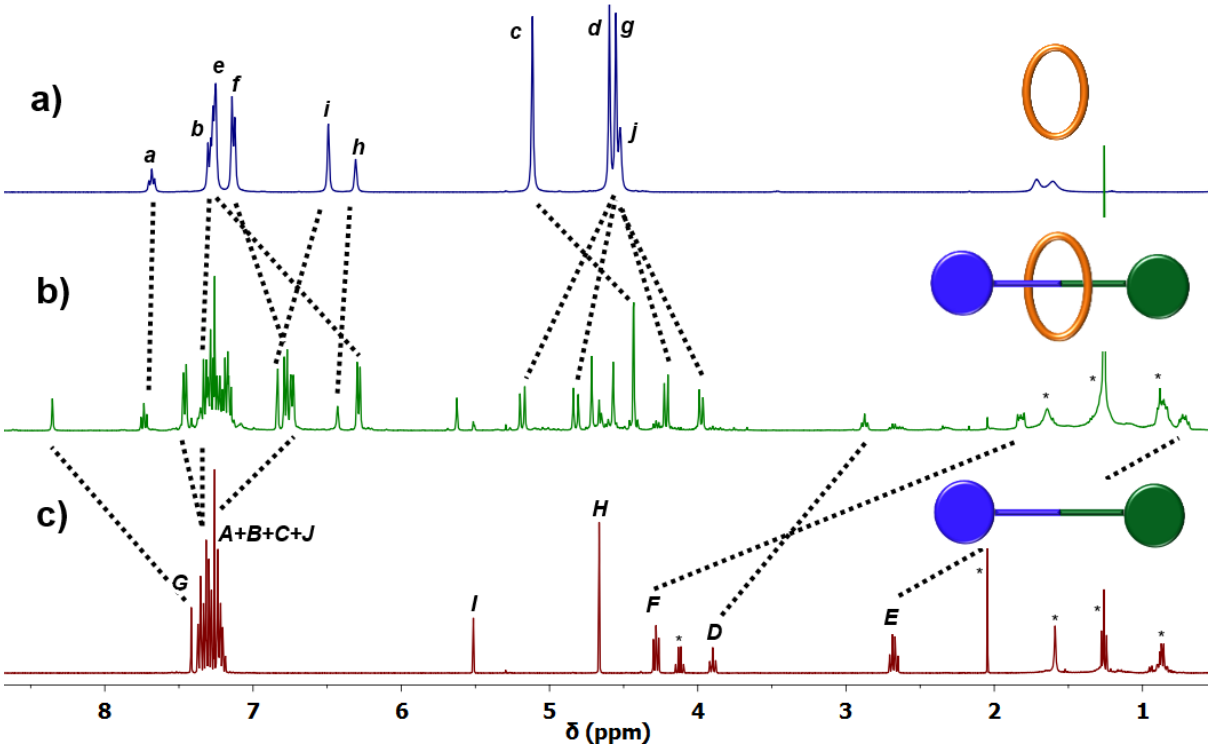

Figure S18. Partial stacked ^{1}H NMR spectra (400 MHz, $CDCl_3$, 298 K) of a) macrocycle **5**, b) [2]rotaxane **11** and c) corresponding 1,2,3-triazole thread (* peaks due to grease, ethyl acetate and *n*-hexane).

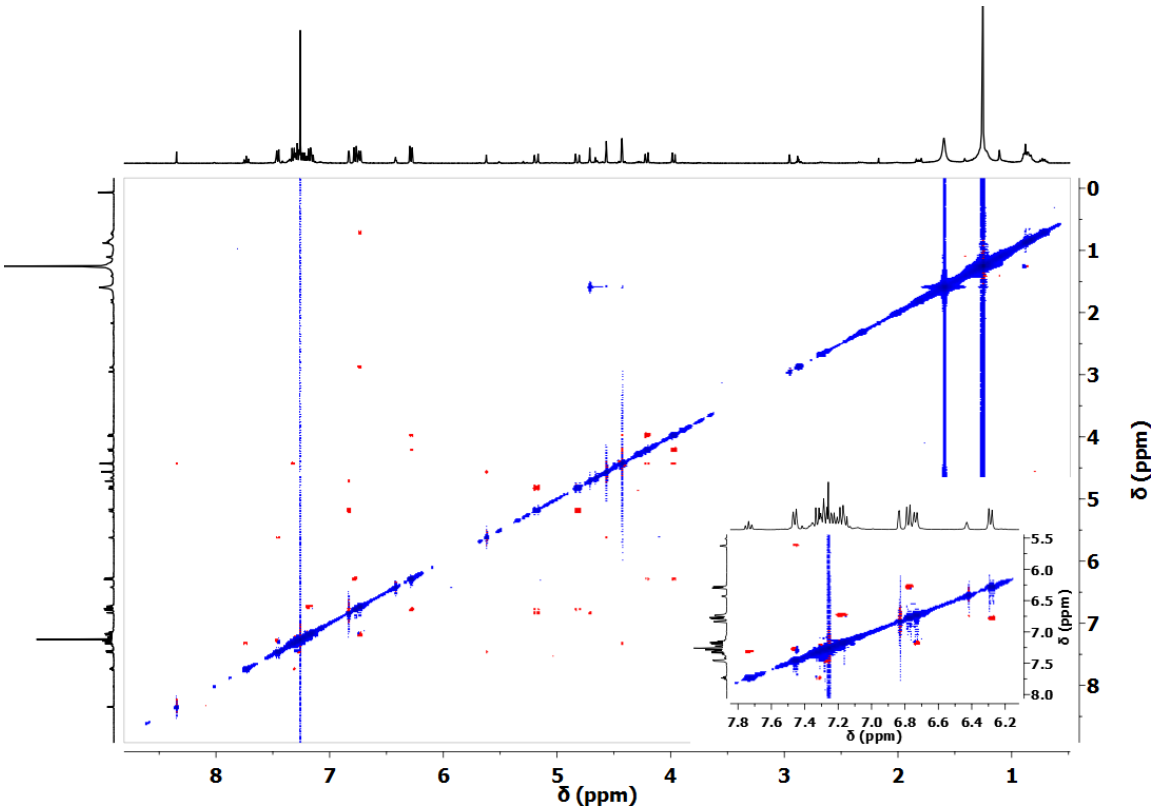

Figure S19. ^{1}H NOESY NMR spectrum (400 MHz, $CDCl_3$, 298 K) of **11**.

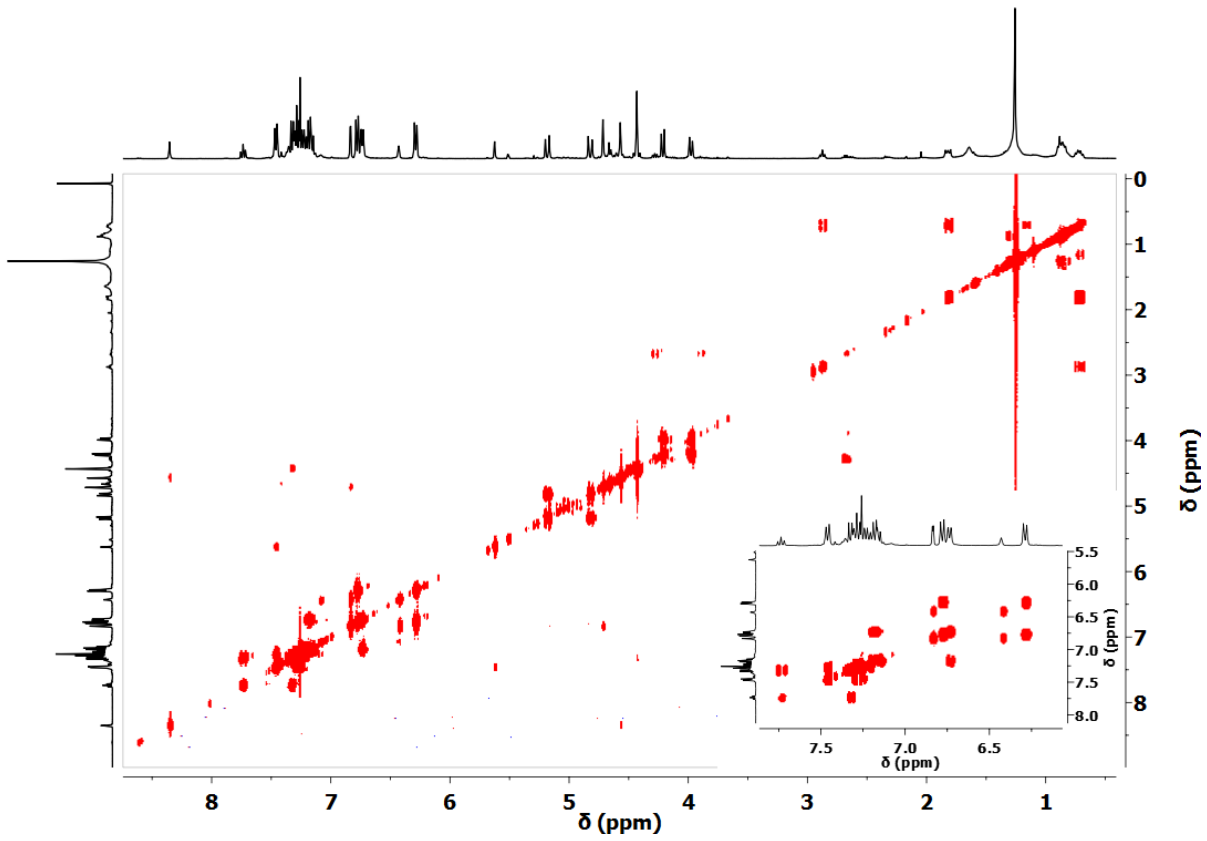

Figure S20. ^{1}H COSY NMR spectrum (400 MHz, $CDCl_3$, 298 K) of **11**.

2.2.3 Attempted Rotaxane 12

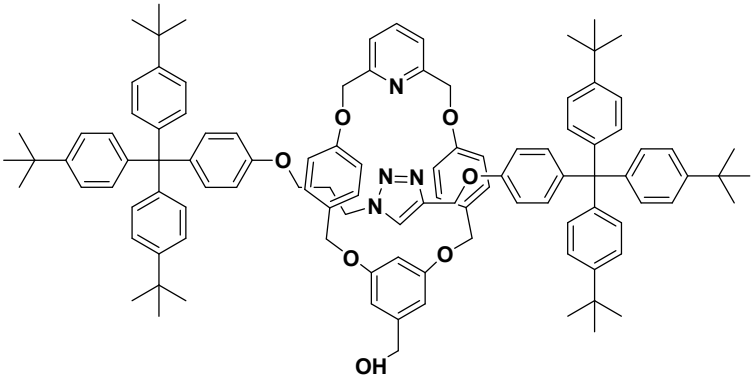

A solution of macrocycle **4** (100 mg, 0.227 mmol) and $[Cu(CH_3CN)_4](PF_6)$ (90 mg, 0.241 mmol) in dry CH_2Cl_2 (20 mL) was stirred under nitrogen for 1 h. Azide **6** (400 mg, 1.756 mmol) and alkyne **7** (320 mg, 1.756 mmol) were then added. The mixture was refluxed for 48 h, then diluted with CH_2Cl_2 (20 mL), and a methanol (20 mL) solution of KCN (143 mg, 2.19 mmol) was added. The resulting suspension was stirred at RT for 2 h and then the solvents

were evaporated by heating the mixture at 80 °C in an oil bath. The residue was partitioned between water (50 mL) and CH_2Cl_2 (75 mL) and the layers were separated. The aqueous layer was extracted with CH_2Cl_2 (2 × 75 mL) and the combined organic layers were washed with water (50 mL) and brine (50 mL). After drying the organic layer over $MgSO_4$, the suspension was filtered and the solvent was removed under reduced pressure. The residue was analysed by HR-ES mass spectroscopy and TLC. No peaks for rotaxane **12** were identified.

2.3 Metal Complexes of Macrocycles

2.3.1 Copper(I) Complex of Macrocycle 4

Macrocycle **4** (12 mg, 0.026 mmol, 1 eq.) and $[Cu(CH_3CN)_4](PF_6)$ (10 mg, 0.026 mmol, 1 eq.) in CD_2Cl_2 (1 mL) were stirred at RT for 1 h to give a copper(I) complex. HR-ESMS: *m/z* = 518.1023 [**4**+Cu]$^+$ (calc. for $C_{286}H_{25}CuNO_5$, 518.1017).

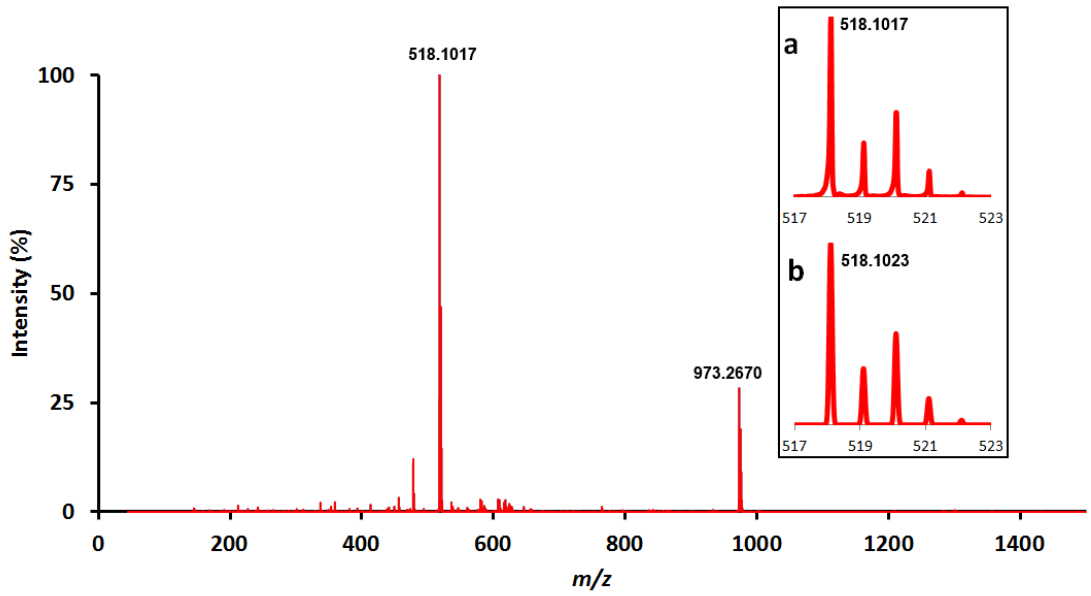

Figure S21. HR-ESMS spectrum of 1:1 mixture of **4** and $[Cu(CH_3CN)_4](PF_6)$, inset a) observed and b) calculated isotopic patterns for [**4**+Cu]$^+$ at *m/z* = 518.1017. The peak at *m/z* = 973.2670 is due to [(**4**)$_2$+Cu]$^+$ ions.

2.3.2 Silver(I) Complex of Macrocycle 4

Macrocycle **4** (9 mg, 0.02 mmol, 1 eq.) and AgOTf (5 mg, 0.02 mmol, 1 eq.) in methanol (5 mL) were stirred in the absence of light to give a silver(I) complex. HR-ESMS: *m/z* = 564.0778 [**4**+Ag]$^+$ (calc. for $C_{28}H_{25}AgNO_5$, 564.0755).

Colourless crystals of [(**4**)Ag(**4**)](OTf) suitable for X-ray crystallography were obtained by vapour diffusion of diethyl ether into a methanolic solution of the complex (*vide infra*).

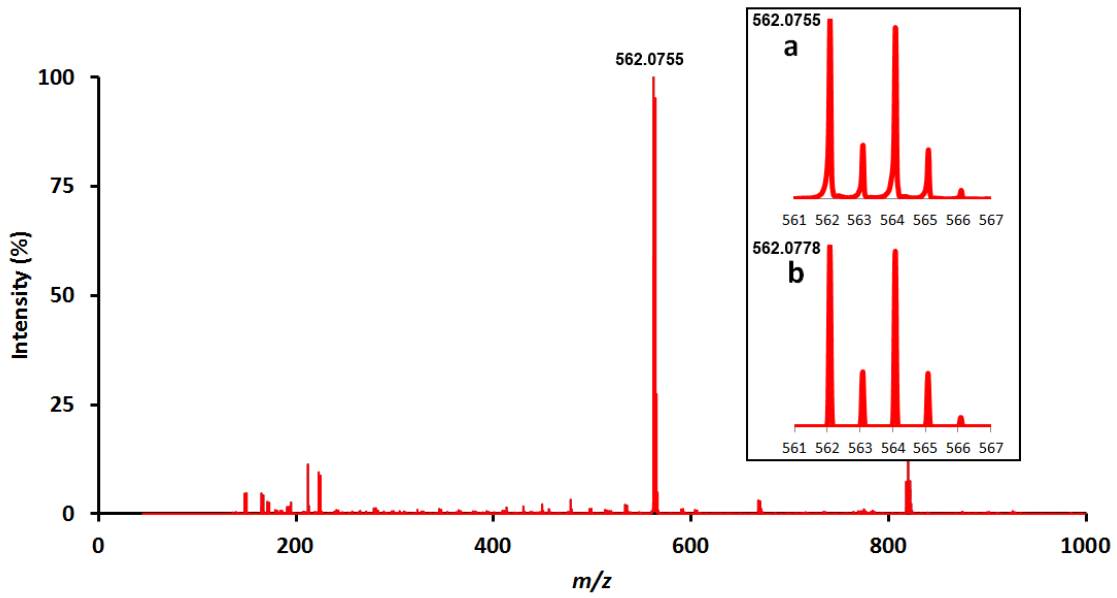

Figure S22. HR-ESMS spectrum of 1:1 mixture of **4** and Ag(OTf), inset a) observed and b) calculated isotopic patterns for [**4**+Ag]$^+$ at *m/z* = 562.0755.

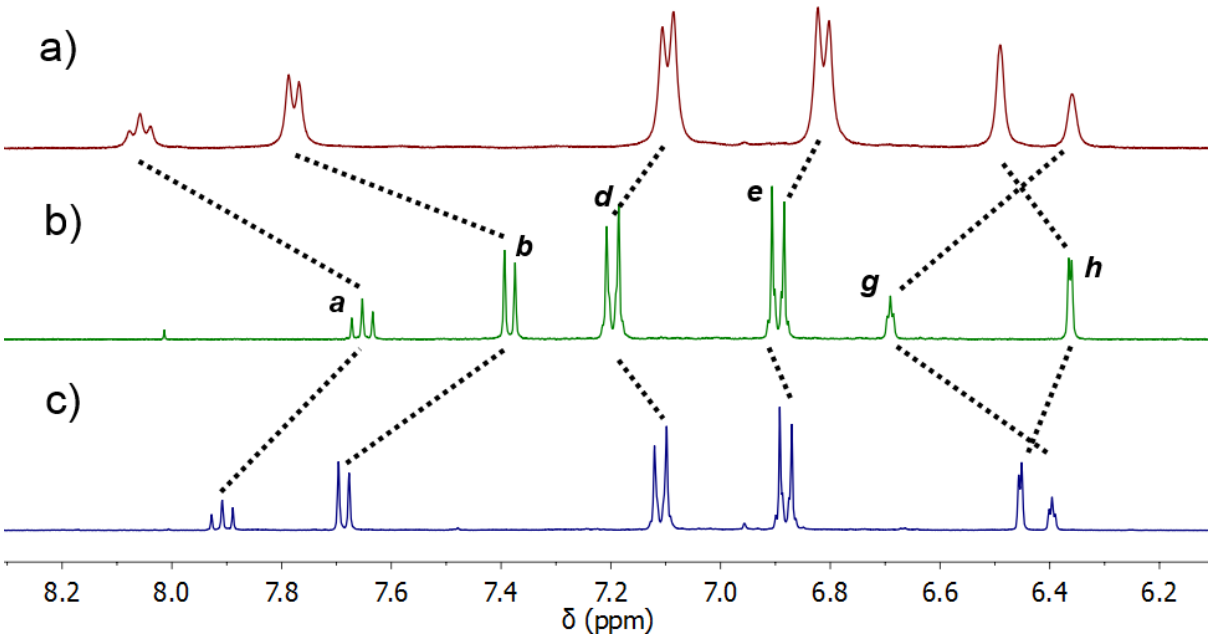

Figure S23. Partial stacked ^{1}H NMR spectra (400 MHz, acetone-d_6, 298 K) of a) a 1:1 mixture of **4** and [Cu(CH$_3$CN)$_4$](PF$_6$), b) macrocycle **4** and c) a 1:1 mixture of **4** and AgOTf.

2.3.3 Copper(I) Complex of Macrocycle 5

Macrocycle **5** (25 mg, 0.052 mmol, 1 eq.) and $[Cu(CH_3CN)_4](PF_6)$ (13 mg, 0.052 mmol, 1 eq.) in CD_3CN (10 mL) were stirred for 1 h to give a copper(I) complex. HR-ESMS: *m/z* = 546.1336 [**5**+Cu]$^+$ (calc. for $C_{30}H_{29}CuNO_5$, 546.1309).

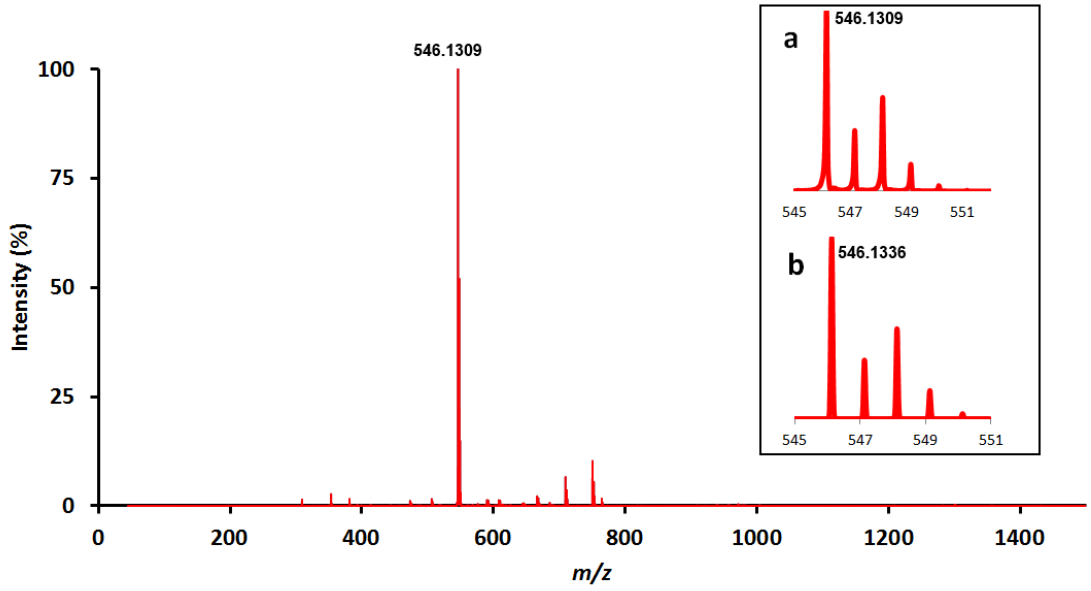

Figure S24. HR-ESMS spectrum of 1:1 mixture of **5** and $[Cu(CH_3CN)_4](PF_6)$ inset a) observed and b) calculated isotopic patterns for [**5**+Cu]$^+$ at *m/z* = 546.1309.

2.3.4 Silver(I) Complex of Macrocycle 5

Macrocycle **5** (40 mg, 0.077 mmol, 1 eq.) and AgOTf (20 mg, 0.077 mmol, 1 eq.) in methanol (5 mL) were stirred in the absence of light to give a silver(I) complex. HR-ESMS: *m/z* = 592.1089 [**5**+Ag]$^+$ (calc. for $C_{30}H_{29}AgNO_5$, 592.1062).

Colourless crystals of [(**5**)Ag(**5**)](OTf) suitable for X-ray crystallography were obtained by vapour diffusion of diethyl ether into a methanolic solution of the silver(I) complex (*vide infra*).

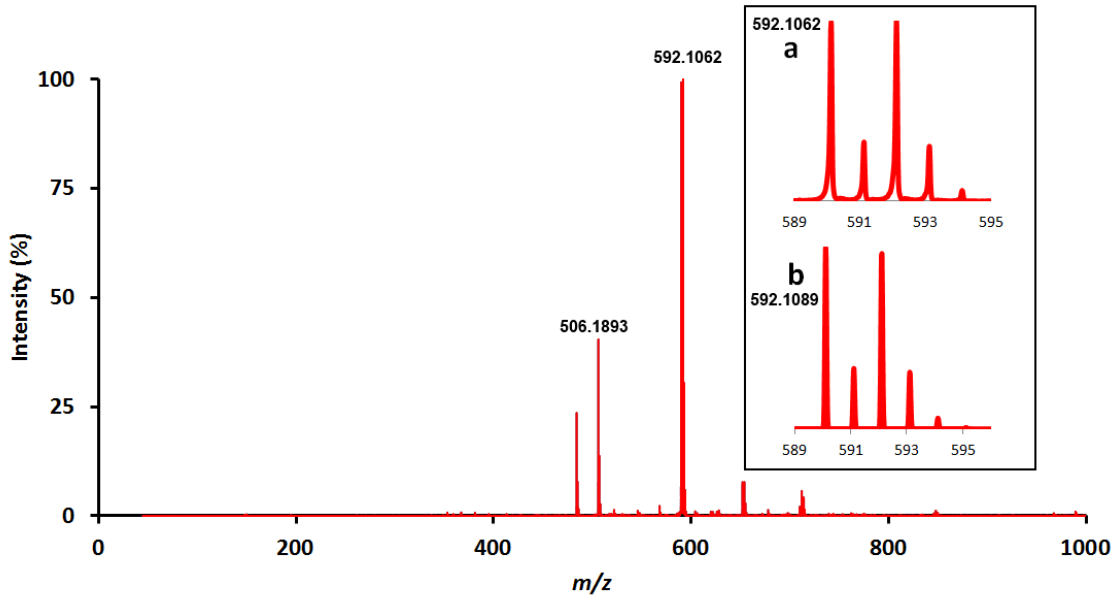

Figure S25. HR-ESI-MS spectrum of 1:1 mixture of **5** and Ag(OTf), inset a) observed and b) calculated isotopic patterns for [**5**+Ag]$^+$ at *m/z* = 592.1062. Also showing peaks due to [**5**+H]$^+$ ions at *m/z* = 506.1893.

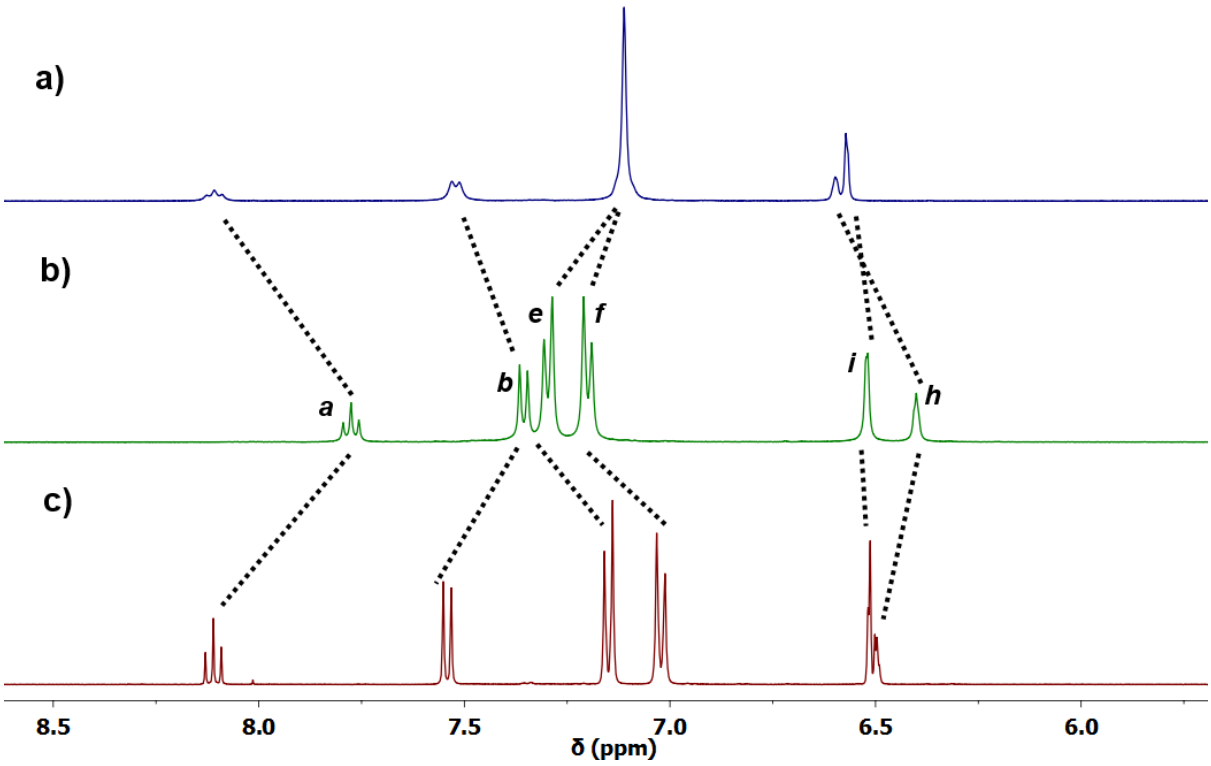

Figure S26. Partial stacked ^{1}H NMR spectra (400 MHz, acetone-d_6, 298 K) of a) a 1:1 mixture of **5** and [Cu(CH$_3$CN)$_4$](PF$_6$), b) macrocycle **5** and c) a 1:1 mixture of **5** and AgOTf.

2.3.5 Silver(I) Complex of Rotaxane 11, $[Ag_2(11)_2](OTf)_2$

Rotaxane **11** (20 mg, 0.021 mmol, 1 eq.) and AgOTf (6 mg, 0.02 mmol, 1 eq.) were dissolved in methanol (5 mL) and stirred in the absence of light to give $[Ag_2(\mathbf{11})_2](OTf)_2$. ^{1}H NMR (500 MHz, acetone-d_6) δ 8.35 (s, 1H, H_G), 7.95 – 7.79 (m, 1H, H_a), 7.44 – 7.41 (m, 4H), H_J, 7.35 – 7.13 (m, 14H, H_A, H_B, H_K, H_L, H_b), 6.96 (d, J = 2.2 Hz, 2H, H_i), 6.84 – 6.49 (m, 8H, $H_{aromatic}$), 6.27 – 6.09 (m, 5H, $H_{aromatic}$), 5.35 (s, 1H, H_I), 5.12 – 4.89 (m, 6H, H_g, H_j), 4.82 – 4.67 (m, 6H, H_H, H_c), 4.45 – 4.27 (m, 4H, H_d), 3.46 – 3.25 (m, 2H, H_F), 2.78 (t, 1H, H_D), 1.11 (t, J = 7.0 Hz, 2H, H_E); HR-ESMS: *m/z* = 1051.3402 [**11**+Ag]$^+$ (calc. for $C_{61}H_{58}AgN_4O_6$, 1051.3482) and *m/z* = 1993.7762 [(**11**)$_2$+Ag]$^+$ (calc. for $C_{122}H_{116}N_8O_{12}Ag$, 1993.7971); Anal. calc. for $C_{62}H_{58}AgF_3N_4O_9S$: C, 62.05; H, 4.87; N, 4.67; found: C, 61.99; H, 5.01, N, 4.69.

Colourless crystals of $[Ag_2(\mathbf{11})_2](OTf)_2$ suitable for X-ray crystallography were obtained by vapour diffusion of diethyl ether into a methanolic solution of the silver(I) complex (*vide infra*).

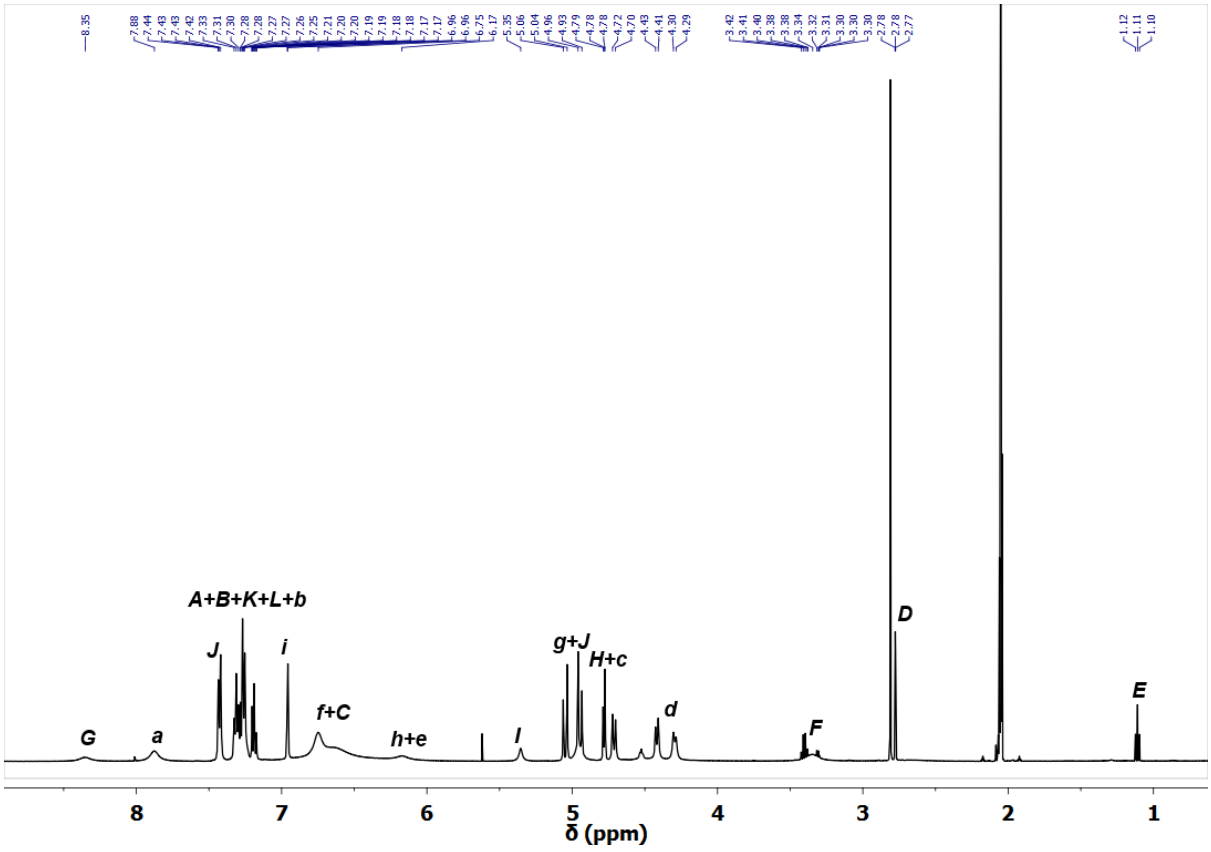

Figure S27. ^{1}H NMR spectrum (400 MHz, acetone-d_6, 298 K) of $[Ag_2(\mathbf{11})_2](OTf)_2$ (peaks are assigned according to rotaxane **11**).

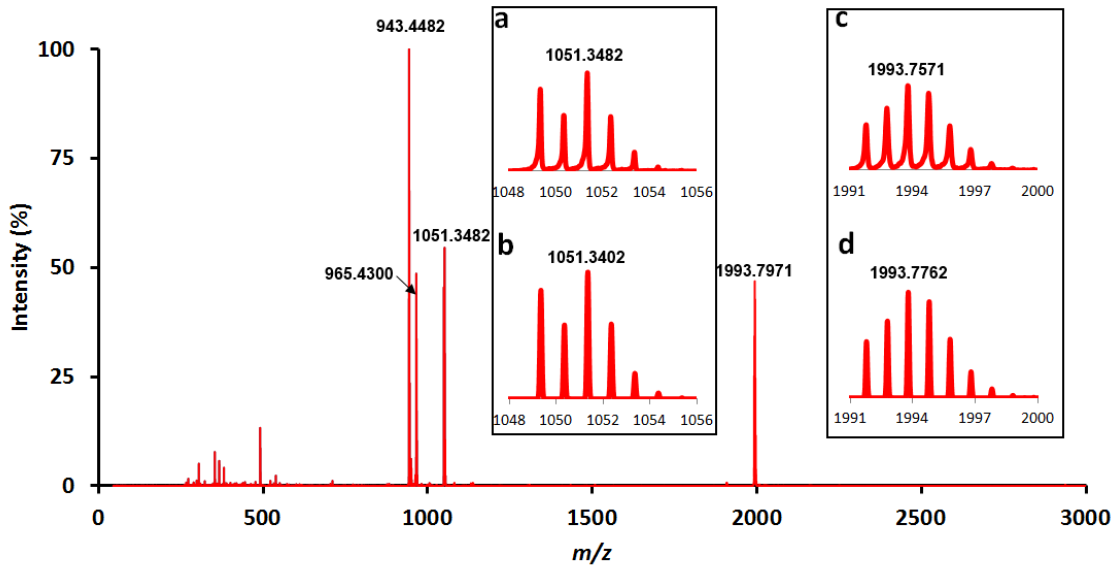

Figure S28. HR-ESMS spectrum of the complex $[Ag_2(\mathbf{11})_2](OTf)_2$, insets a) observed and b) calculated isotopic patterns for $[\mathbf{11}+Ag]^+$ at m/z = 1051.3482 and c) observed and d) calculated isotopic patterns for $[(\mathbf{11})_2+Ag]^+$ at m/z = 1993.7571. Also showing peaks due to $[\mathbf{11}+H]^+$ and $[\mathbf{11}+Na]^+$ at m/z = 943.4482 and 965.4300.

3 Selected ^{1}H DOSY Spectra

Table S1. Diffusion coefficients obtained from ^{1}H DOSY NMR (500 MHz, acetone-d_6) experiments.

Species	D ($\times 10^{-10}$ m^2 s^{-1})
5	11.36
8	3.39
1,2,3-triazole thread in **11**	11.27
11	9.36
$[Ag_2(\mathbf{11})_2](OTf)_2$	7.56

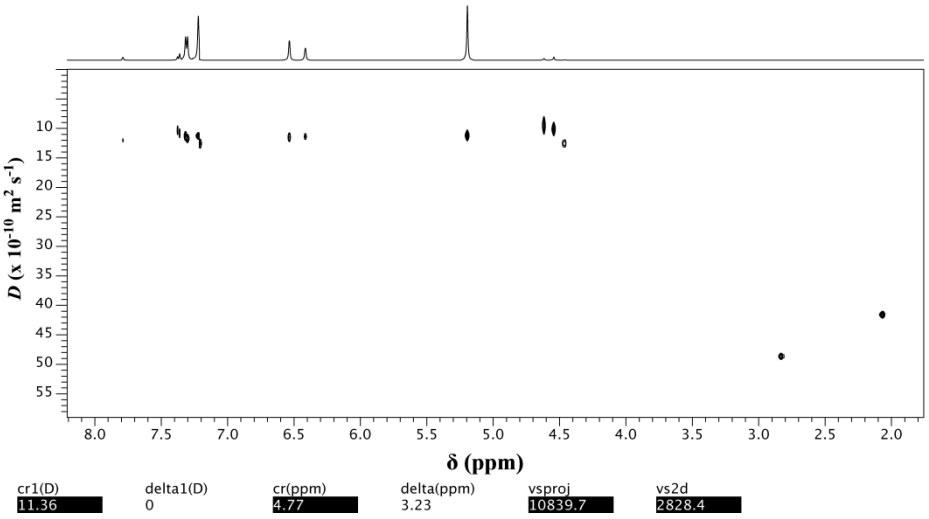

Figure S29. ^{1}H DOSY NMR spectrum (500 MHz, acetone-d_6, 298K) of **5**.

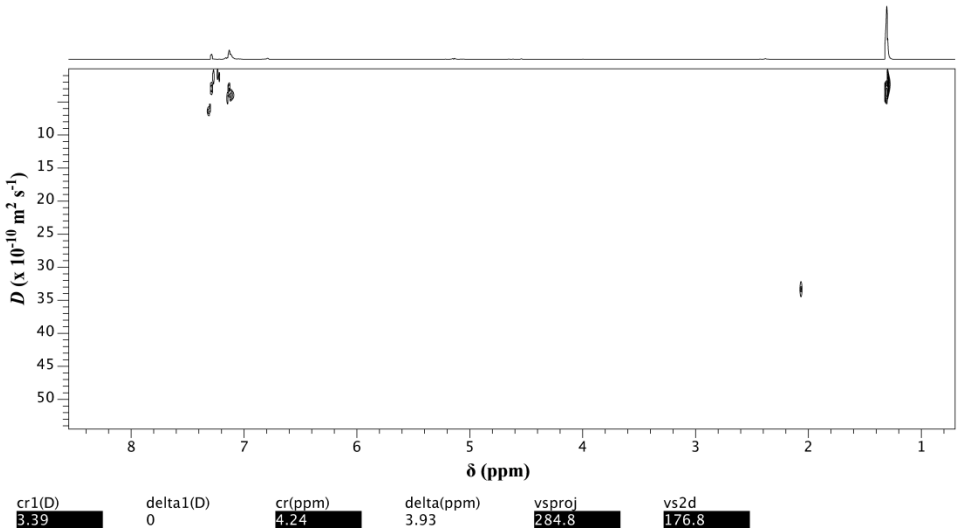

Figure S30. ^{1}H DOSY NMR spectrum (500 MHz, acetone-d_6, 298K) of **8**.

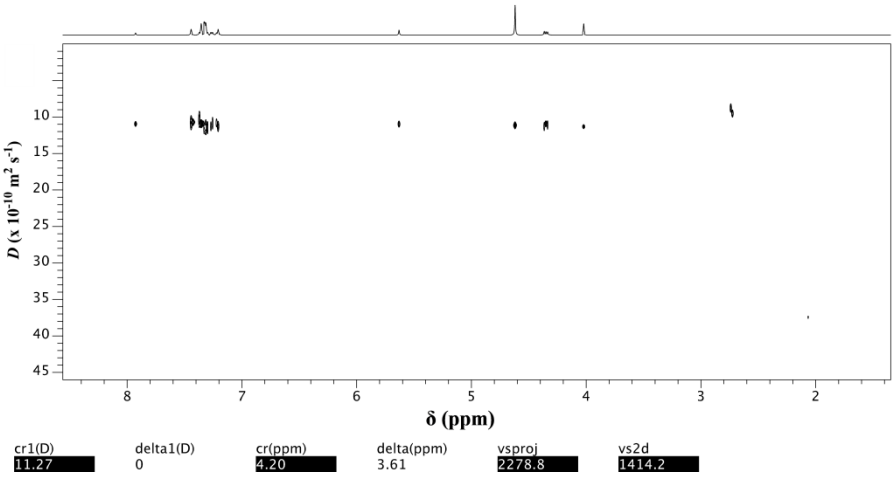

Figure S31. ^{1}H DOSY NMR spectrum (500 MHz, acetone-d_6, 298K) of the 1,2,3-triazole thread component of rotaxane **11**.

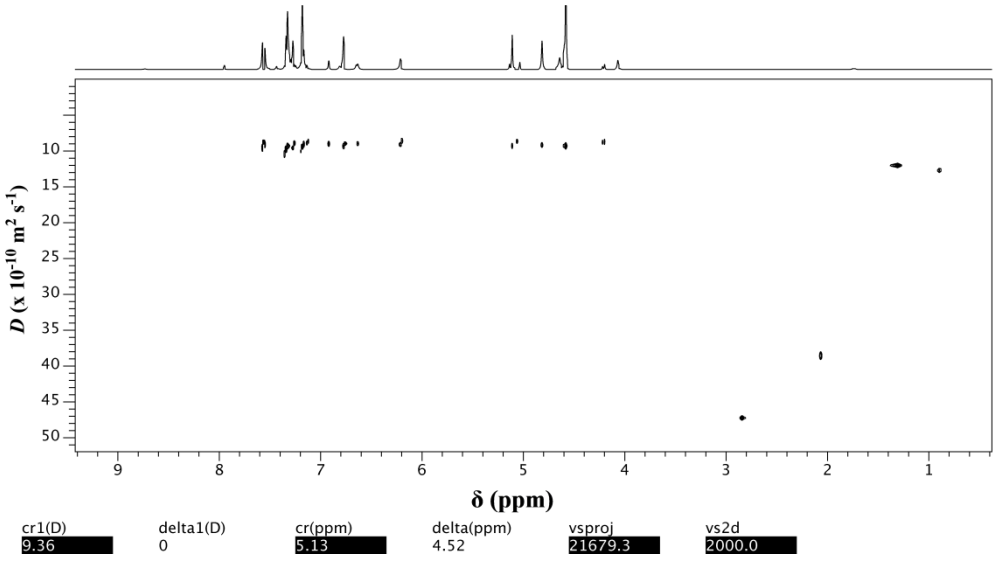

Figure S32. ^{1}H DOSY NMR spectrum (500 MHz, acetone-d_6, 298K) of rotaxane **11**.

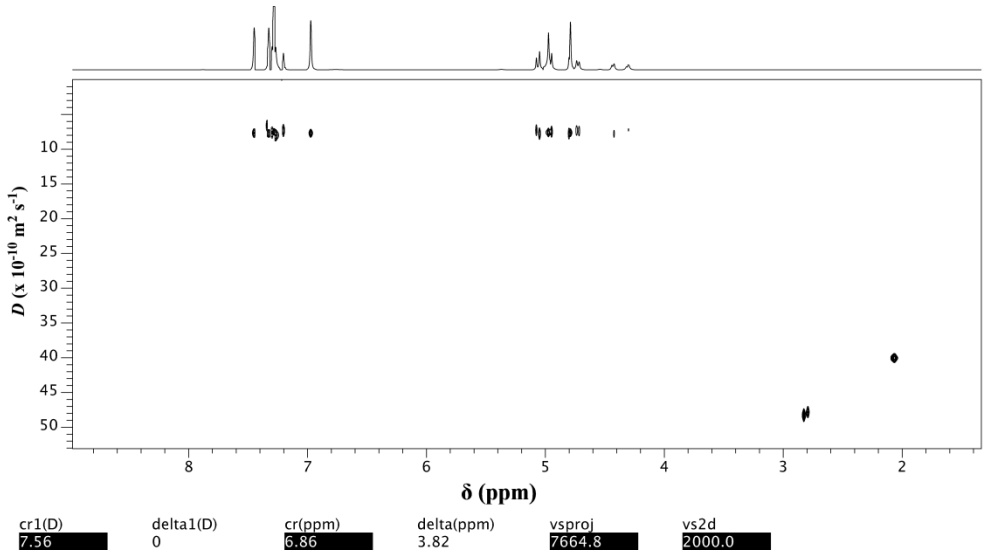

Figure S33. ^{1}H DOSY NMR spectrum (500 MHz, acetone-d_6, 298K) of the complex $[Ag_2(\mathbf{11})_2](OTf)_2$.

4 X-ray Crystallography

4.1 Data Collection

X-ray data for the macrocycle **4**, macrocycle **5**, [(**4**)Ag(**4**)](OTf), [(**5**)Ag(**5**)](OTf) and $[Ag_2(\mathbf{11})_2](OTf)_2$ was collected at 100 K on an Agilent Technologies Supernova system using Cu Kα radiation, and data were treated using CrysAlisPro[5] software. The structures were solved using either SIR-97[6] or SHELXS-97[7] and weighted full-martix refinement on F^2 was carried out using SHELXL-97[7] running within either the WinGX[8] package or the xSeed[9] program.

4.2 Data Refinement for macrocycle 4

All non-hydrogen atoms were refined anisotropically. Hydrogen atoms were placed in calculated positions and refined using a riding model. The structure was solved in the monoclinic space group $P2_1/n$ and refined to an R_1 value of 4.6%. The asymmetric unit contains one macrocycle **4** molecule.

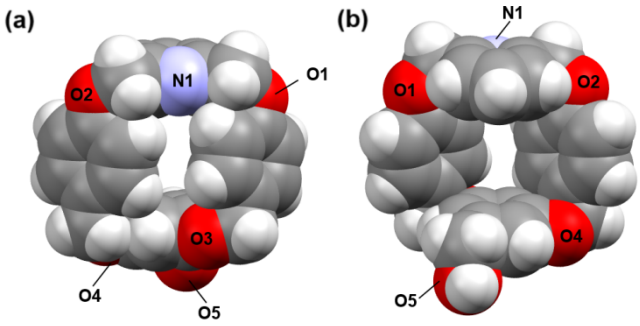

Figure S34. Labelled space filling diagrams (a) and (b) of **4** showing the macrocyclic cavity.

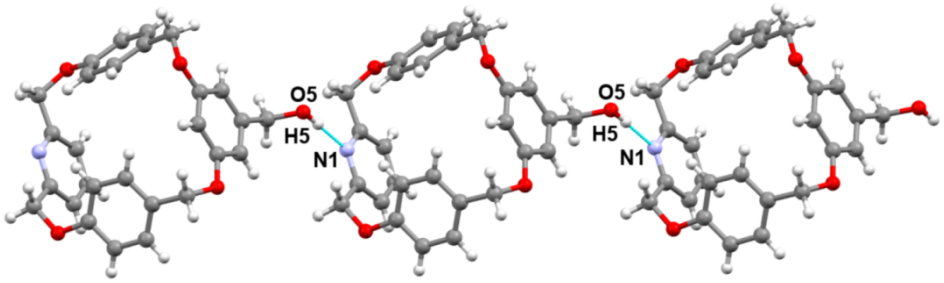

Figure S35. Labelled ball-and-stick diagram of a linear supramolecular chain formed by hydrogen bonding between alcohol OH proton and pyridyl N (N1---O5 2.776(2) Å, O5-H5---N1 170.7(1)°) of macrocycle **4** molecules.

4.3 Data Refinement for macrocycle 5

All non-hydrogen atoms were refined anisotropically. Hydrogen atoms were placed in calculated positions and refined using a riding model. The structure was solved in the triclinic space group $P\bar{1}$ and refined to an R_1 value of 3.9%. The asymmetric unit contains one macrocycle **5** molecule.

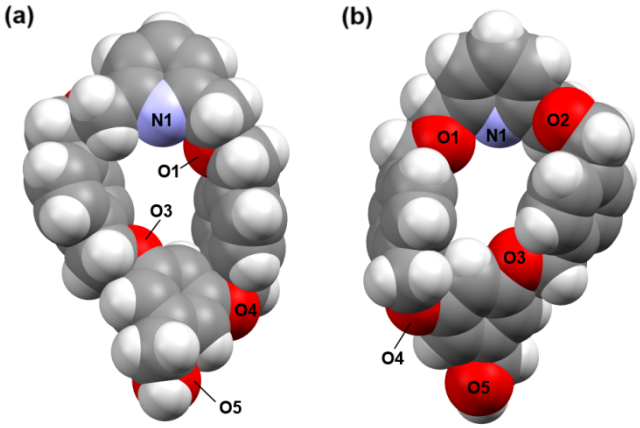

Figure S36. Labelled space filling diagrams (a) and (b) of **5** showing the macrocyclic cavity.

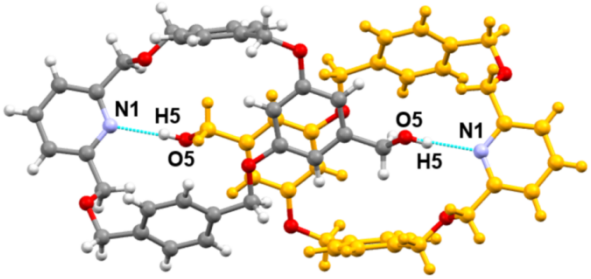

Figure S37. Labelled ball-and-stick diagram of a dimer formed by **5**. Hydrogen bonding between alcohol OH proton and pyridyl N atom (N1---O5 2.841(2) Å, O5-H5---N1 170.69(8)°) generates the dimer.

4.4 Data Refinement for [(4)Ag(4)](OTf)

All non-hydrogen atoms were refined anisotropically. Hydrogen atoms were placed in calculated positions and refined using a riding model. The structure was solved in the monoclinic space group *Pn* and refined to an R_1 value of 3.6%. The asymmetric unit contains two crystallographically independent [(**4**)Ag(**4**)]$^+$ cations and two triflate anions. The two macrocycles in a [(**4**)Ag(**4**)]$^+$ cation are also crystallographically independent (Figure S37).

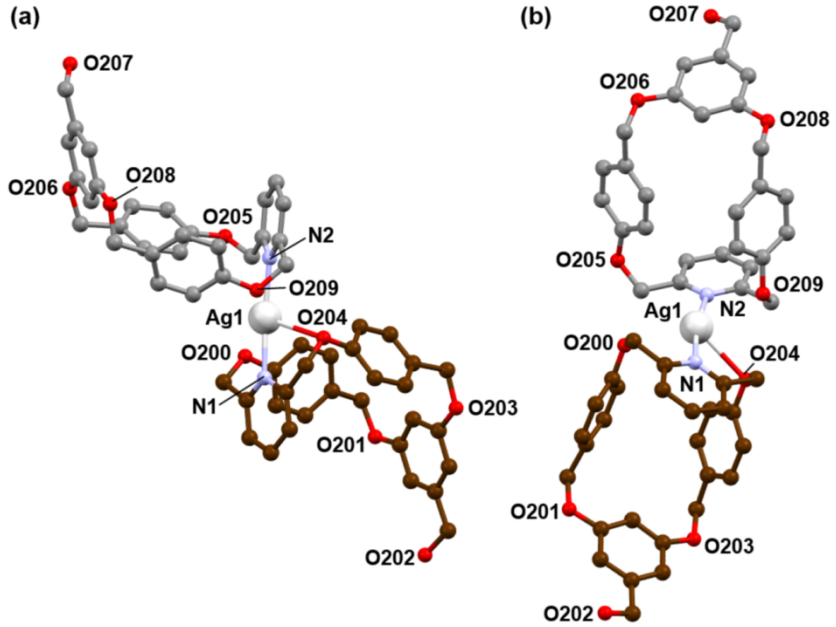

Figure S38. Labelled ball-and-stick diagrams (a) and (b) of a [(**4**)Ag(**4**)]$^+$ cation; hydrogen atoms are omitted for clarity. Selected distances (Å) and angles (°): Ag1-N1 2.224(3), Ag1-N2 2.210(3), N1-Ag1-N2 171.3(1). The two macrocycles in a [(**4**)Ag(**4**)]$^+$ cation are crystallographically independent, and were coloured in grey and brown.

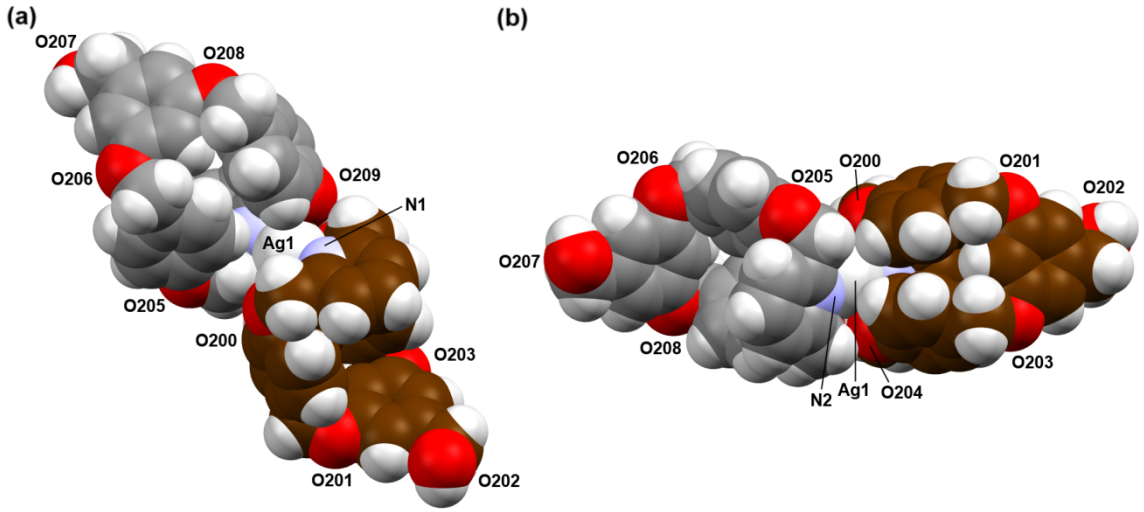

Figure S39. Labelled space filling diagrams (a) and (b) of a [(**4**)Ag(**4**)]$^+$ cation showing the Ag(I) ion is surrounded by two coordinated macrocyclic ligands. The two macrocycles in a [(**4**)Ag(**4**)]$^+$ cation are crystallographically independent, and were coloured in grey and brown.

4.5 Data Refinement for [(5)Ag(5)](OTf)

All non-hydrogen atoms were refined anisotropically. Hydrogen atoms were placed in calculated positions and refined using a riding model. The structure was solved in the triclinic space group $P\bar{1}$ and refined to an R_1 value of 4.2%. The asymmetric unit contains one half of two crystallographically independent [(**5**)Ag(**5**)]$^+$ cations, where both Ag atoms are 50% occupancies, and one triflate anion.

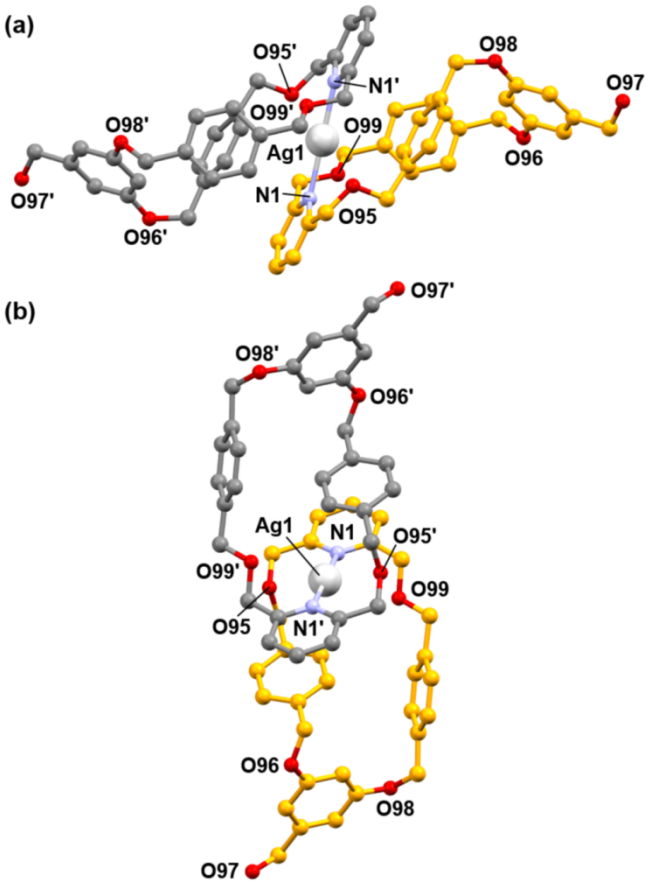

Figure S40. Labelled ball-and-stick diagrams (a) and (b) of a [(**5**)Ag(**5**)]$^{+}$ cation; hydrogen atoms are omitted for clarity. Selected distances (Å) and angles (°): Ag1-N1 2.224(2), N1-Ag1-N1′ 180.00(6).

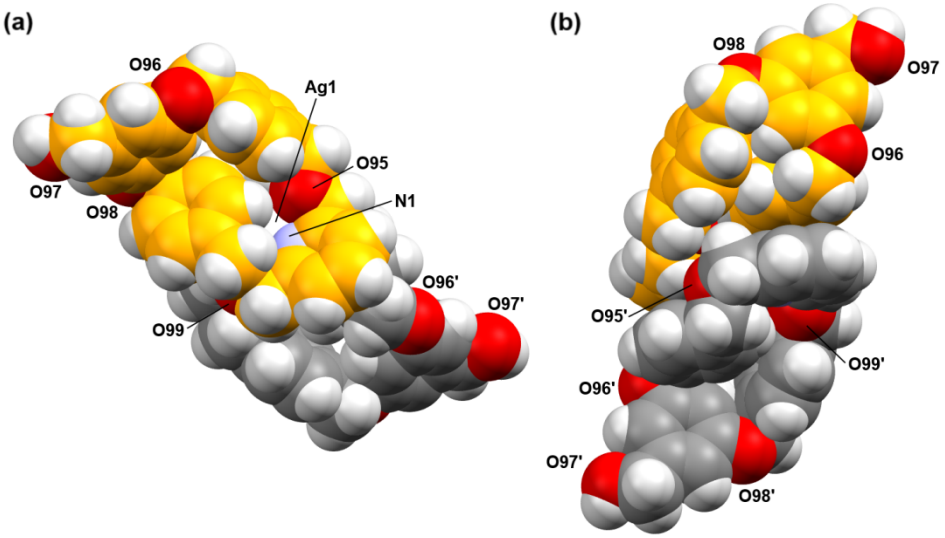

Figure S41. Labelled space filling diagrams (a) and (b) of a [(**5**)Ag(**5**)]$^{+}$ cation showing the Ag(I) ion is buried by the two coordinated macrocyclic ligands.

4.6 Data Refinement for $[Ag_2(11)_2](OTf)_2$

Bad reflections (−1, −1, 3 and 0, 0, 2) were omitted with the OMIT command. All non-hydrogen atoms were refined anisotropically. Hydrogen atoms were placed in calculated positions and refined using a riding model. The structure was solved in the triclinic space group $P\bar{1}$ and refined to an R_1 value of 5.9%. The asymmetric unit contains a triflate anion and half of a bis-([2]rotaxane) dimer cation $[Ag_2(\mathbf{11})_2]^{2+}$, where the Ag(I) ion is coordinated to a pyridyl N atom and the less electron-rich 1,2,3-triazyol N atom from the same rotaxane and the more electron-rich 1,2,3-triazyol N atom of the other rotaxane.

The trifalte anion was disordered over two sites. The triflate anion was determined to have occupancy of 50% in each site, and was modelled with the same occupancies using the PART command. In addition, the disordered triflate anion was modeled with rigid-body modelling; a combination of DFIX, SADI and ISOR commands were used.

The crystal lattice contained a small amount of diffuse electron density that could not be appropriately modelled. The SQUEEZE routine within PLATON was employed to resolve this problem, resulting in a void electrons count of 33 that we assign to two disordered solvent methanol molecules (36 electrons).

Table S2. SQUEEZE results for $[Ag_2(\mathbf{11})_2](OTf)_2$.

Platon squeeze void average x	0.500
Platon squeeze void average y	0.000
Platon squeeze void average z	0.500
Platon squeeze void volume	229
Platon squeeze void count electrons	33
Platon squeeze details	Disordered solvent methanol molecules that could not be appropriately modelled.

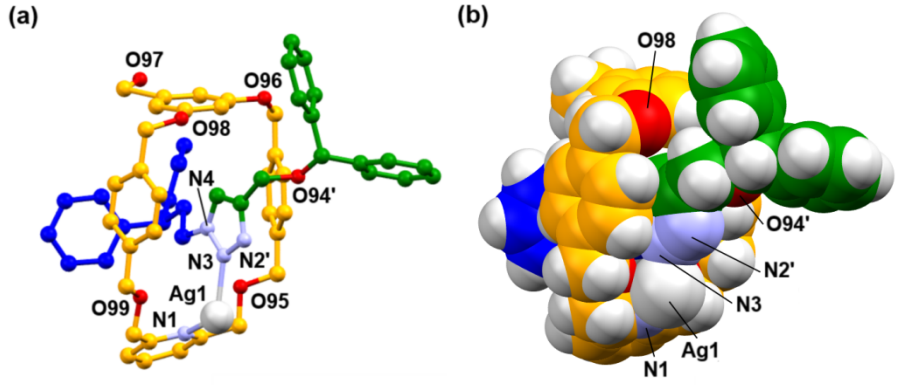

Figure S42. Labelled ball-and-stick (a) and space filling (b) diagrams of half of the bis-([2]rotaxane) dimer cation $[Ag_2(\mathbf{11})_2]^{2+}$.

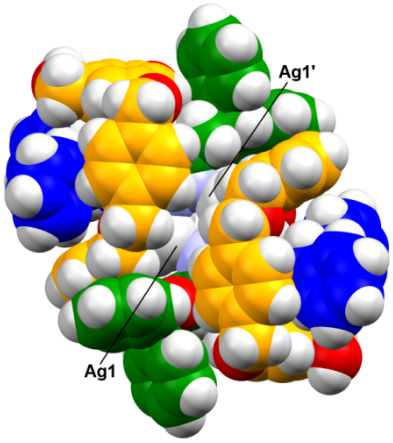

Figure S43. Space filling diagram of a bis-([2]rotaxane) dimer cation $[Ag_2(\mathbf{11})_2]^{2+}$.

4.7 Crystallographic Data for Macrocycles, Ag Macrocycle Complexes and Bis-([2]rotaxane) Dimer

Table S3. Crystallographic data for macrocycle **4** and macrocycle **5**.

	4	**5**
CCDC reference number	997798	997799
empirical formula	$C_{28}H_{25}NO_5$	$C_{30}H_{29}NO_5$
formula weight	455.49	483.54
temperature (K)	100.0(1)	100.0(2)
wavelength (Å)	1.5418	1.5418
crystal system	monoclinic	triclinic
space group	$P2_1/n$	$P\bar{1}$
a (Å)	11.3483(3)	10.9095(3)
b (Å)	13.1679(3)	11.1519(3)
c (Å)	14.9704(3)	11.6650(4)
α (deg)	90	76.633(3)
β (deg)	103.528(2)	88.947(3)
γ (deg)	90	63.197(3)
volume (Å^3)	2175.01(9)	1226.35(6)
Z	4	2
calculated density (Mg m^{-3})	1.391	1.309
absorption coefficient (mm^{-1})	0.777	0.719
crystal size (mm^3)	0.24 x 0.21 x 0.18	0.25 x 0.21 x 0.13
reflections collected	13529	19310
independent reflections (R_{int})	4527 (0.0361)	5111 (0.0269)
data / restraints / parameters	4527/0/308	5111/0/326
goodness-of-fit on F^2	1.140	1.431
final *R* indices [$I > 2\sigma(I)$]	$R_1 = 0.0464$, $wR_2 = 0.1338$	$R_1 = 0.0393$, $wR_2 = 0.1580$
final *R* indices (all data)	$R_1 = 0.0603$, $wR_2 = 0.1385$	$R_1 = 0.0421$, $wR_2 = 0.1628$
largest diff. peak/hole	0.539 and −0.257	0.287 and −0.231

Table S4. Crystallographic data for [(**4**)Ag(**4**)](OTf) and [(**5**)Ag(**5**)](OTf).

	[(4)Ag(4)](OTf)	**[(5)Ag(5)](OTf)**
CCDC reference number	997800	997801
empirical formula	$C_{57}H_{50}AgF_3N_2O_{13}S$	$C_{61}H_{58}AgF_3N_2O_{13}S$
formula weight	1167.92	1224.02
temperature (K)	100.0(1)	100.0(2)
wavelength (Å)	1.5418	1.5418
crystal system	monoclinic	triclinic
space group	*Pn*	$P\bar{1}$
a (Å)	11.04160(10)	12.3931(3)
b (Å)	21.5483(2)	12.7490(3)
c (Å)	21.3436(2)	19.1316(2)
α (deg)	90	106.432(2)
β (deg)	91.7631(9)	90.948(2)
γ (deg)	90	108.504(2)
volume (Å^3)	5075.83(8)	2730.58(10)
Z	4	2
calculated density (Mg m^{-3})	1.528	1.489
absorption coefficient (mm^{-1})	4.265	3.991
crystal size (mm^3)	0.23 x 0.16 x 0.06	0.44 x 0.32 x 0.23
reflections collected	42325	41324
independent reflections (R_{int})	16754 (0.0406)	11399 (0.0415)
data / restraints / parameters	16754/2/1391	11399/0/735
goodness-of-fit on F^2	0.957	1.037
final *R* indices [$I > 2\sigma(I)$]	$R_1 = 0.0360$, $wR_2 = 0.0895$	$R_1 = 0.0416$, $wR_2 = 0.1133$
final *R* indices (all data)	$R_1 = 0.0389$, $wR_2 = 0.0934$	$R_1 = 0.0423$, $wR_2 = 0.1142$
largest diff. peak/hole	0.822 and −0.392	0.670 and −1.341

Table S5. Crystallographic data for $[Ag_2(\mathbf{11})_2](OTf)_2$.

CCDC reference number	997802
empirical formula	$C_{124}H_{116}Ag_2F_6N_8O_{18}S_2$
formula weight	2400.11
temperature (K)	100.0(1)
wavelength (Å)	1.5418
crystal system	triclinic
space group	$P\bar{1}$
a (Å)	11.7502(4)
b (Å)	15.4683(5)
c (Å)	17.5738(3)
α (deg)	108.091(2)
β (deg)	101.907(2)
γ (deg)	98.189(3)
volume (Å^3)	2896.75(15)
Z	1
calculated density (Mg m^{-3})	1.376
absorption coefficient (mm^{-1})	3.708
crystal size (mm^3)	0.33 x 0.22 x 0.19
reflections collected	34617
independent reflections (R_{int})	12033 (0.0417)
data / restraints / parameters	12033/140/795
goodness-of-fit on F^2	0.884
final *R* indices [$I > 2\sigma(I)$]	$R_1 = 0.0591$, $wR_2 = 0.1733$
final *R* indices (all data)	$R_1 = 0.0612$, $wR_2 = 0.1775$
largest diff. peak/hole	1.241 and −1.016

References

1. Y. Zhou, G. Gao, H. Li and J. Qu, *Tetrahedron Lett.*, 2008, **49**, 3260-3263.
2. X. Li, T. G. Upton, C. L. D. Gibb and B. C. Gibb, *J. Am. Chem. Soc.*, 2002, **125**, 650-651.
3. P. Rajakumar, M. Dhanasekaran, S. Selvam, P. G. Aravindan and D. Velmurugan, *J. Org. Chem*, 2005, **70**, 3267-3270.
4. S. Braese, C. Gil, K. Knepper and V. Zimmermann, *Angew. Chem., Int. Ed.*, 2005, **44**, 5188-5240.
5. CrysAlisPro, *Agilent Technologies: Yarnton, Oxfordshire, England, 2012*.
6. A. Altomare, M. C. Burla, M. Camalli, G. L. Cascarano, C. Giacovazzo, A. Guagliardi, A. G. G. Moliterni, G. Polidori and R. Spagna, *J. Appl. Cryst.*, 1999, **32**, 115-119.
7. G. Sheldrick, *Acta Cryst.*, 2008, **A64**, 112-122.
8. L. Farrugia, *J. Appl. Cryst.*, 1999, **32**, 837-838.
9. L. J. Barbour, *J. Supramol. Chem.*, 2001, **1**, 189-191.